# STUDIES ON SILAR DEPOSITED $Sn_XS_Y$ FILMS WITH VARYING Sn (Tin) to S (Sulphur) RATIO

**THESIS**

**SUBMITTED IN PARTIAL FULFILLMENT OF THE REQUIREMENT FOR THE AWARD OF THE DEGREE OF**

**MASTER OF TECHNOLOGY**
**IN**
**ENERGY SCIENCE & TECHNOLOGY**

**Submitted by**


**VISHVAJEET CHANDRA DEY**
**EXAM Roll No-M4ENR19014**


**UNDER**
**SUPERVISION OF**


**Dr. RATAN MANDAL** **Dr. SUBRATA DAS**



**Course affiliated to**
**FACULTY OF ENGINEERING AND TECHNOLOGY**
**Under**
**FACULTY OF INTER DISCIPLINARY STUDIES, LAW & MANAGEMENT**
**JADAVPUR UNIVERSITY**
**KOLKATA-700032**
**2019**

M Tech Energy Science and Technology
Course affiliated to
Faculty Council of Interdisciplinary Studies Law and Management
Jadavpur University
Kolkata ,India

# BONAFIDE CERTIFICATE

Certified that this thesis report **STUDIES ON SILAR DEPOSITED $Sn_XS_Y$ FILMS WITH VARYING Sn (Tin) to S (Sulphur) RATIO** is the bonafide work of **VISHVAJEET CHANDRA DEY (Examination Roll No. – M4ENR19014, Registration No.: 143091 of 2017-2018),** who carried out the thesis work under my supervision. Certified further, that to the best of my knowledge the work reported herein does not form part of any other thesis report or dissertation on the basis of which a degree or award was conferred on an earlier occasion on this or any other candidate. I hereby recommend that the thesis be accepted in partial fulfillments for *Post Graduate Degree* of **Master of Technology** in **Energy Science & Technology** during the academic session 2017-19.

……

**Dr. SUBRATA DAS**
**THESIS SUPERVISOR**

SCHOOL OF ENERGY STUDIES
JADAVPUR UNIVERSITY
KOLKATA - 700032

……

**Dr. RATAN MONDAL**
**THESIS SUPERVISOR**
DIRECTOR
SCHOOL OF ENERGY STUDIES
JADAVPUR UNIVERSITY
KOLKATA - 700032

……

**Prof. PANKAJ KUMAR ROY**
**DEAN**
Faculty Council of Interdisciplinary Studies, Law & Management
Jadavpur University
Kolkata – 700032

FACULTY COUNCIL OF INTERDISCIPLINARY STUDIES LAW & MANAGEMENT
JADAVPUR UNIVERSITY
KOLKATA,INDIA

# CERTIFICATE OF APPROVAL

The forgoing thesis is hereby approved as a creditable study of a technological subject carried out and presented in a manner satisfactory to warrant its acceptance as a perquisite to the *Post Graduate Degree* of **Master of Technology in Energy Science & Technology** for which it has been submitted. It is understood that by this approval the undersigned person does not necessarily endorse or approve any statement made, opinion expressed or conclusion drawn therein but approve the thesis only for the purpose for which it has been submitted.

_____

_____

Committee of final examination for Evaluation of Thesis

# CANDIDATE'S DECLARATION

I hereby certify that the work which is being presented in the thesis entitled "STUDIES ON SILAR DEPOSITED $Sn_XS_Y$ FILMS WITH VARYING Sn (Tin) to S (Sulphur) RATIO" by "VISHVAJEET CHANDRA DEY" in partial fulfillment of requirements for the award of degree of M.Tech. in Energy Science & Technology submitted in the Department of School of Energy Studies at JADAVPUR UNIVERSITY, KOLKATA, is an authentic record of my own work carried out during a period from 2018 to 2019 under the supervision of Dr. Subrata Das and Dr. Ratan Mandal. The matter presented in this thesis has not been submitted by me in any other University / Institute for the award of M.Tech. Degree.

All information in this document have been obtained and presented in accordance with academic rules and ethical conduct.

I also declare that as required by these rules and conduct, I have fully cited and referenced all materials and results that are not original to this work.

**NAME:** VISHVAJEET CHANDRA DEY

**EXAM ROLL NO.:** M4ENR19014

**THESIS TITLE:** STUDIES ON SILAR DEPOSITED $Sn_XS_Y$ FILMS WITH VARYING Sn (Tin) to S (Sulphur) RATIO

**SIGNATURE:**

**DATE:**

**Dedicated**
**To**
**My family**
**And**
**My Classmates**

# ACKNOWLEDGEMENT

I would like to place on record my deep sense of gratitude to Dr. Subrata Das, School of Energy Studies, Jadavpur University, Kolkata, India for his generous guidance, help and useful suggestions.

I express my sincere gratitude to Prof. Ratan Mandal, School of Energy Studies, Jadavpur University, Kolkata, India, for his stimulating guidance, continuous encouragement and supervision throughout the course of present work.

I also wish to extend my thanks to Prof. Tushar Jash and other colleagues for attending my seminars and for their insightful comments and constructive suggestions to improve the quality of this research work.

I would like to thank all my friends, seniors, juniors and fellow classmates who supported me and encouraged me all time.

Last but not the least, I would like to thank my parents and my grandparents for moral encouragement and all family members for their support.

# CONTENTS

# LIST OF FIGURES

# 1. INTRODUCTION

## 1.1Introduction

Solar cells have always been aligned closely with other electronic devices. The basic aspects of semiconductor materials and the physical mechanisms which are at the center of photovoltaic devices are described here. These physical mechanisms are used to explain the operation of a p-n junction, which forms the basis not only for the great majority of solar cells, but also most other electronic devices such as lasers and bipolar junction transistors. Much of the theory of solid-state semiconductors was worked out during the invention of the transistor in the late 40's and early 50s. While PV semiconductor materials are not limited to silicon, the dominance of silicon in the PV market has led to our particular emphasis of that material for the PVCDROM.

## 1.2 Semiconductor Material

The atoms in a semiconductor are materials from either group IV of the periodic table, or from a combination of group III and group V (called III-V semiconductors), or of combinations from group II and group VI (called II-VI semiconductors). Because different semiconductors are made up of elements from different groups in the periodic table, properties vary between semiconductors. Silicon, which is a group IV, is the most commonly used semiconductor material as it forms the basis for integrated circuit (IC) chips and is the most mature technology and most solar cells are also silicon based.

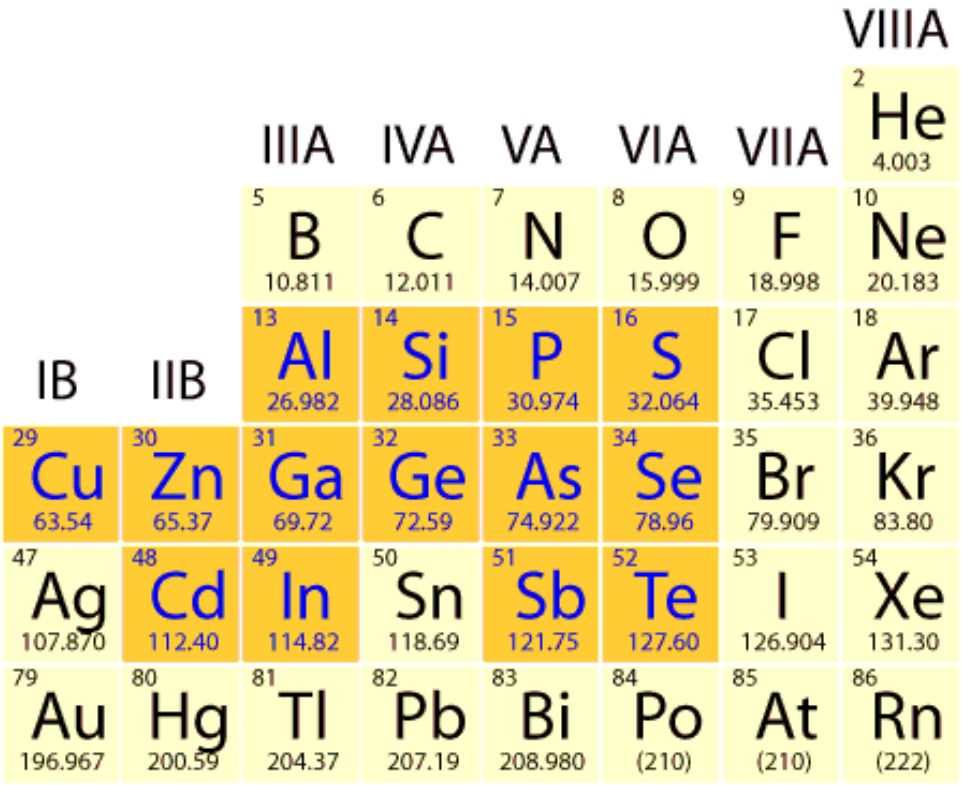


**Fig. 1** Section from the periodic table.

More common semiconductor materials are shown in dark box colour in fig. 1. A semiconductor can be either of a single element, such as Si or Ge, a compound, such as GaAs, InP or CdTe, or an alloy, such as $Si_xGe_{(1-x)}$ or $Al_xGa_{(1-x)}As$, where x is the fraction of the particular element and ranges from 0 to 1.

### 1.3 Semiconductor structure

Semiconductors, such as Silicon (Si) are made up of individual atoms bonded together in a regular, periodic structure to form an arrangement whereby each atom is surrounded by 8 electrons. An individual atom consists of a nucleus made up of a core of protons (positively charged particles) and neutrons (particles having no charge) surrounded by electrons. The number of electrons and protons is equal, such that the atom is overall electrically neutral. The electrons surrounding each atom in a semiconductor are part of a covalent bond. A covalent bond consists of two atoms "sharing" a single electron. Each atom forms 4 covalent bonds with the 4 surrounding atoms. Therefore, between each atom and its 4 surrounding atoms, 8 electrons are being shared. The structure of a semiconductor is shown in the figure below.

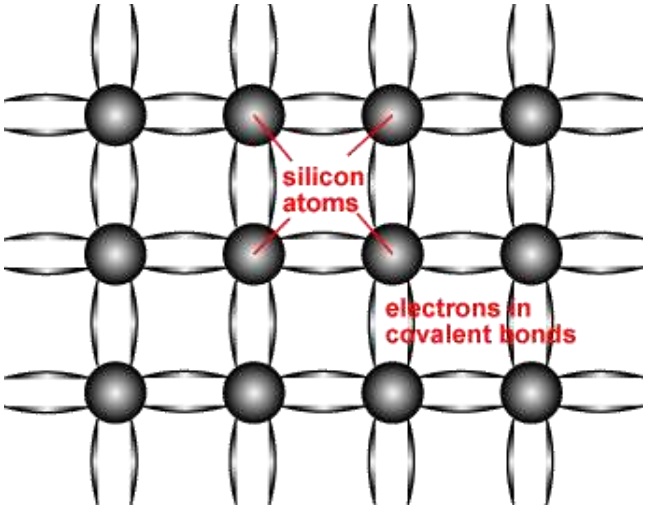


**Fig. 2.**

Fig. 2.shows schematic representation of covalent bonds in a silicon crystal lattice. Each line connecting the atoms represents an electron being shared between the two. Two electrons being shared are what form the covalent bond.

### 1.4 Conduction in Semiconductors

The bond structure of a semiconductor determines the material properties of a semiconductor. One key effect is the energy levels which the electrons can occupy and how they move about the crystal lattice. The electrons in the covalent bond formed between each of the atoms in the lattice structure are held in place by this bond and hence they are localized to the region surrounding the atom. These bonded electrons cannot move or change energy, and thus are not considered "free" and cannot participate in current flow, absorption, or other physical processes of interest in solar cells. However, only at absolute zero are all electrons in this "stuck," bonded arrangement. At elevated temperatures, especially at the temperatures where solar cells operate, electrons can gain enough energy to escape from their bonds. When this happens, the electrons are free to move about the crystal lattice and participate in conduction. At room temperature, a semiconductor has enough free electrons to allow it to conduct current. At or close to absolute zero a semiconductor behaves like an insulator.

When an electron gains enough energy to participate in conduction (is "free"), it is at a high energy state. When the electron is bound, and thus cannot participate in conduction, the electron is at a low energy state. Therefore, the presence of the bond between the two atoms introduces two distinct energy states for the electrons. The electron cannot attain energy values

intermediate to these two levels; it is either at a low energy position in the bond, or it has gained enough energy to break free and therefore has a certain minimum energy. This minimum energy is called the "band gap" of a semiconductor. The number and energy of these free electrons, those electrons participating in conduction, is basic to the operation of electronic devices.

The space left behind by the electrons allows a covalent bond to move from one electron to another, thus appearing to be a positive charge moving through the crystal lattice. This empty space is commonly called a "hole", and is similar to an electron, but with a positive charge.

The most important parameters of a semiconductor material for solar cell operation are:

- The band gap;
- The number of free carriers (electrons or holes) available for conduction; and
- The "generation" and recombination of free carriers (electrons or holes) in response to light shining on the material.

### 1.5 p-n Junction

P-n junctions are formed by joining n-type and p-type semiconductor materials, as shown below. Since the n-type region has a high electron concentration and the p-type a high hole concentration, electrons diffuse from the n-type side to the p-type side. Similarly, holes flow by diffusion from the p-type side to the n-type side. If the electrons and holes were not charged, this diffusion process would continue until the concentration of electrons and holes on the two sides were the same, as happens if two gasses come into contact with each other. However, in a p-n junction, when the electrons and holes move to the other side of the junction, they leave behind exposed charges on dopant atom sites, which are fixed in the crystal lattice and are unable to move. On the n-type side, positive ion cores are exposed. On the p-type side, negative ion cores are exposed. An electric field Ê forms between the positive ion cores in the n-type material and negative ion cores in the p-type material. This region is called the "depletion region" since the electric field quickly sweeps free carriers out, hence the region is depleted of free carriers. A "built in" potential $V_{bi}$ due to Ê is formed at the junction.

## 1.6 Solar Cell

### 1.6.1 Structure

A solar cell is an electronic device which directly converts sunlight into electricity. Light shining on the solar cell produces both a current and a voltage to generate electric power. This process requires firstly, a material in which the absorption of light raises an electron to a higher energy state, and secondly, the movement of this higher energy electron from the solar cell into an external circuit. The electron then dissipates its energy in the external circuit and returns to the solar cell. A variety of materials and processes can potentially satisfy the requirements for photovoltaic energy conversion, but in practice nearly all photovoltaic energy conversion uses semiconductor materials in the form of a p-n junction.

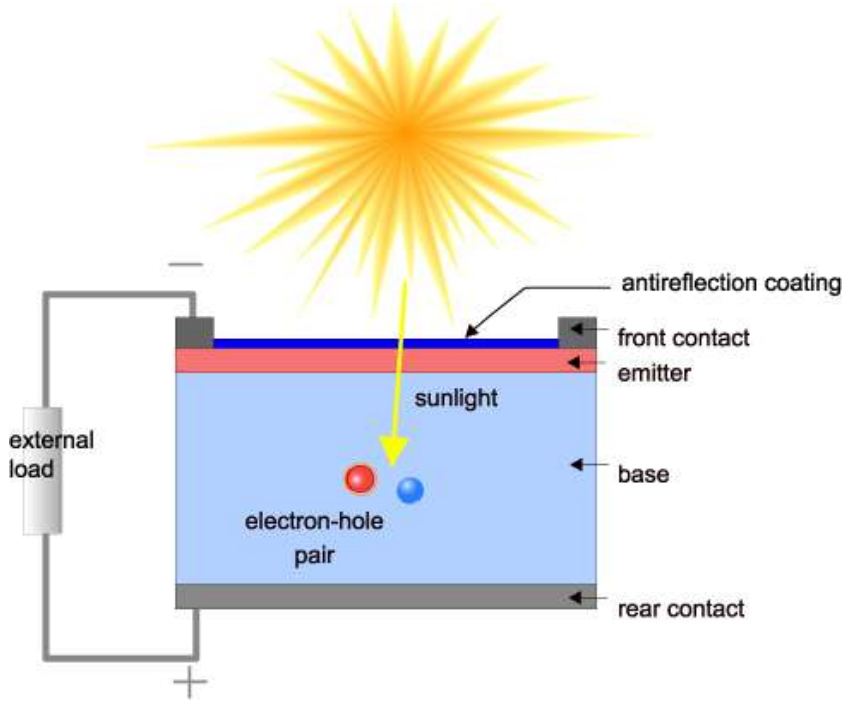


**Fig.3. Cross section of a solar cell.**

The basic steps in the operation of a solar cell are:

- The generation of light-generated carriers;
- The collection of the light-generated carries to generate a current;
- The generation of a large voltage across the solar cell; and
- The dissipation of power in the load and in parasitic resistances.

### 1.6.2 Light Generated Current

The generation of current in a solar cell, known as the "light-generated current", involves two key processes. The first process is the absorption of incident photons to create electron-hole pairs. Electron-hole pairs will be generated in the solar cell provided that the incident photon has energy greater than that of the band gap. However, electrons (in the p-type material), and holes (in the n-type material) are meta-stable and will only exist, on average, for a length of time equal to the minority carrier lifetime before they recombine. If the carrier recombines, then the light-generated electron-hole pair is lost and no current or power can be generated.

A second process, the collection of these carriers by the p-n junction, prevents this recombination by using a p-n junction to spatially separate the electron and the hole. The carriers are separated by the action of the electric field existing at the p-n junction. If the light-generated minority carrier reaches the p-n junction, it is swept across the junction by the electric field at the junction, where it is now a majority carrier. If the emitter and base of the solar cell are connected together (i.e., if the solar cell is short-circuited), the light-generated carriers flow through the external circuit.

### 1.6.3 Solar Cell Parameters

#### a) Short Circuit Current

The short-circuit current is the current through the solar cell when the voltage across the solar cell is zero (i.e., when the solar cell is short circuited). Usually written as $I_{SC}$, the short-circuit current is shown in fig.4.

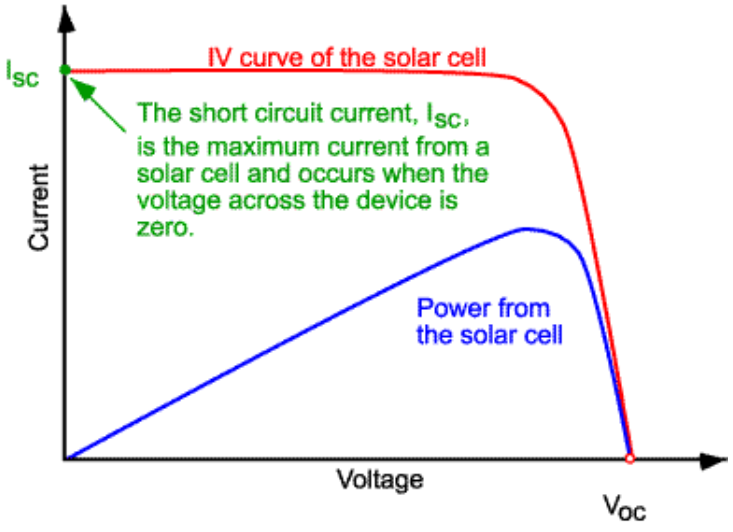


**Fig 4.**

**b) <u>Open Circuit Voltage</u>**

The open-circuit voltage, $V_{OC}$, is the maximum voltage available from a solar cell, and this occurs at zero current. The open-circuit voltage corresponds to the amount of forward bias on the solar cell due to the bias of the solar cell junction with the light-generated current. The open-circuit voltage is shown in fig.5.

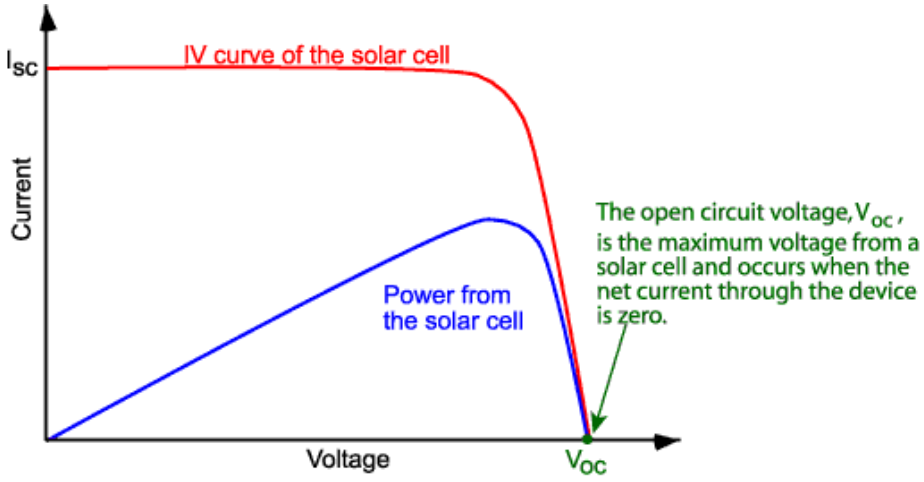


**Fig. 5**

**c) Fill Factor**

The short-circuit current and the open-circuit voltage are the maximum current and voltage respectively from a solar cell. However, at both of these operating points, the power from the solar cell is zero. The "fill factor", more commonly known by its abbreviation "FF", is a parameter which, in conjunction with $V_{oc}$ and $I_{sc}$, determines the maximum power from a solar cell. The FF is defined as the ratio of the maximum power from the solar cell to the product of $V_{oc}$ and $I_{sc}$.

$$FF = \frac{V_{MP}I_{MP}}{V_{OC}I_{SC}}$$

Graphically, the FF is a measure of the "squareness" of the solar cell and is also the area of the largest rectangle which will fit in the IV curve. The FF is illustrated in fig.6.

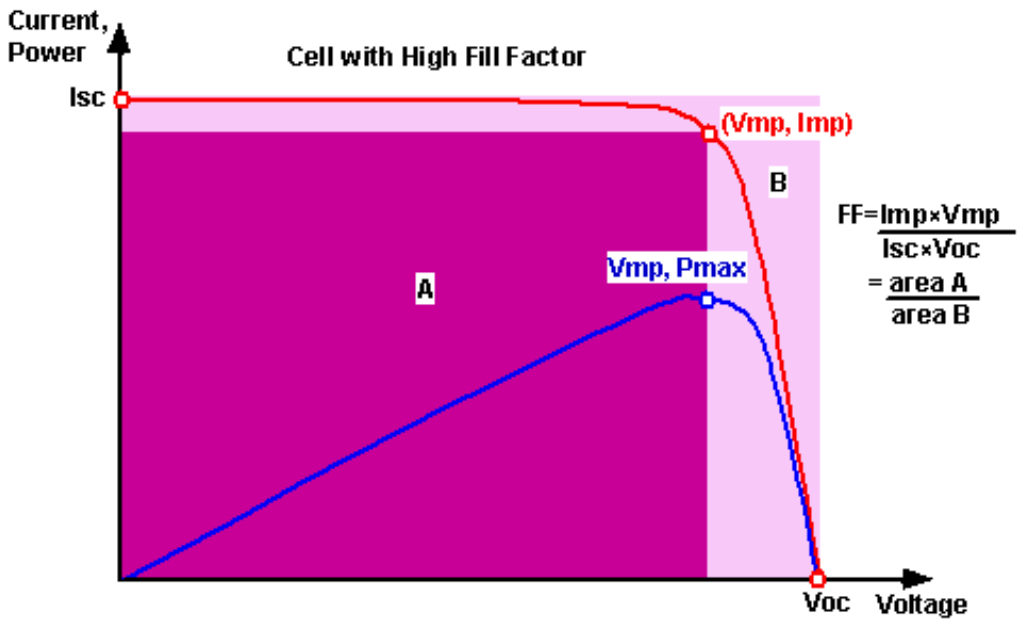


**Fig.6.**

**d) Solar Cell Efficiency**

The efficiency of a solar cell is determined as the fraction of incident power which is converted to electricity and is defined as:

$$P_{max} = V_{OC} I_{SC} FF$$

$$\eta = \frac{V_{OC} I_{SC} FF}{P_{in}}$$

Where:

$V_{OC}$ is the open-circuit voltage;

$I_{SC}$ is the short-circuit current;

FF is the fill factor and

$\eta$ is the efficiency.

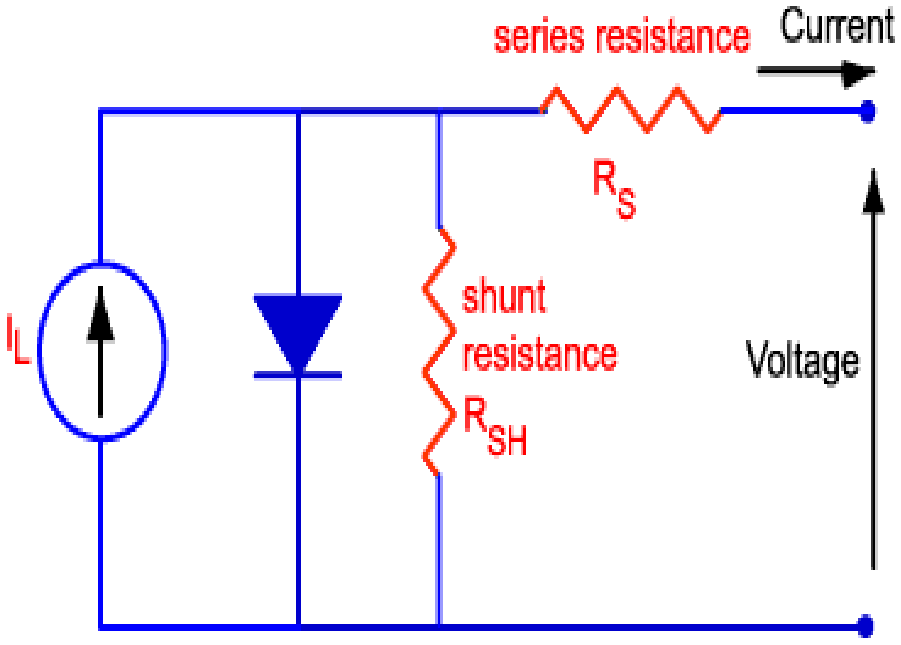


**Fig 7. Equivalent electrical circuit of solar cell**

**e) Series resistance ($R_s$)**

Series resistance of a solar cell occurs due to sheet resistance of semiconductor layers and contact resistance of metal-semiconductor interface. It affects the field factor and short circuit current ($I_{SC}$) largely if metal semiconductor interfacing is not matched properly.

$$R_S = dV/dI \text{ at } V = V_{OC} \text{(Open circuit voltage)}$$

**f) Shunt resistance ($R_{SH}$)**

It arises mainly due to manufacturing defects. $R_{SH}$ is mainly due to leakage current caused by several leakage paths, e.g. recombination of photo generated electrons, surface leakage current at the edges and through n-type contact materials shunting the junction. Low shunt resistance allows an alternate path to the photo current thus minimizing the load current and voltage to keep its value large enough by shuttering down all possible diverse path edge cutting of films are done after fabrication and a special care is taken to remove defect levels of films during fabrication.

$$R_{SH} = dV/dI \text{ at } I = I_{SC} \text{ (Short circuit current)}$$

### 1.7 Overall equation of solar cell

The diode equation of solar cell-

$$I = I_0\left[exp\frac{q(V-IR_s}{nkT} - 1\right] - \frac{V-IR_s}{R_{sh}} - I_L$$

Where

I = output current in amp

$I_L$= photo generated current in amp

$I_0$= reverse saturated current in amp

n=diode ideality factor

K = Boltzmann's constant

T = absolute temperature

Q = charge of carrier

$R_{SH}$= shunt resistance

$R_S$ = series resistance

$I_L$ and $I_0$ are depending on bias voltage temperature. However, for an ideal diode n varies between 1 and 2 and $I_0$ depends only on temperature.

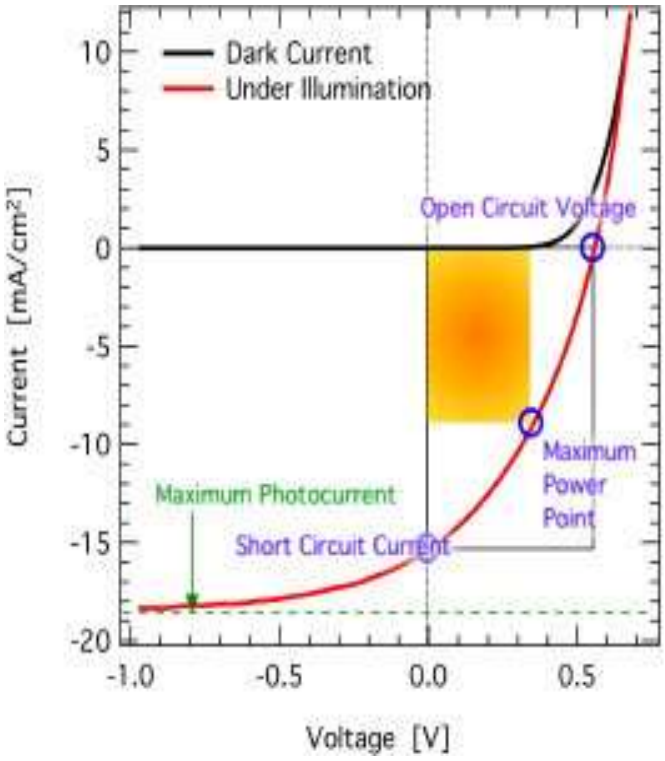


**Fig.8 I-V Characteristics of Solar Cell**

## 1.8 Tandem Cells

One method to increase the efficiency of a solar cell is to split the spectrum and use a solar cell that is optimised to each section of the spectrum.

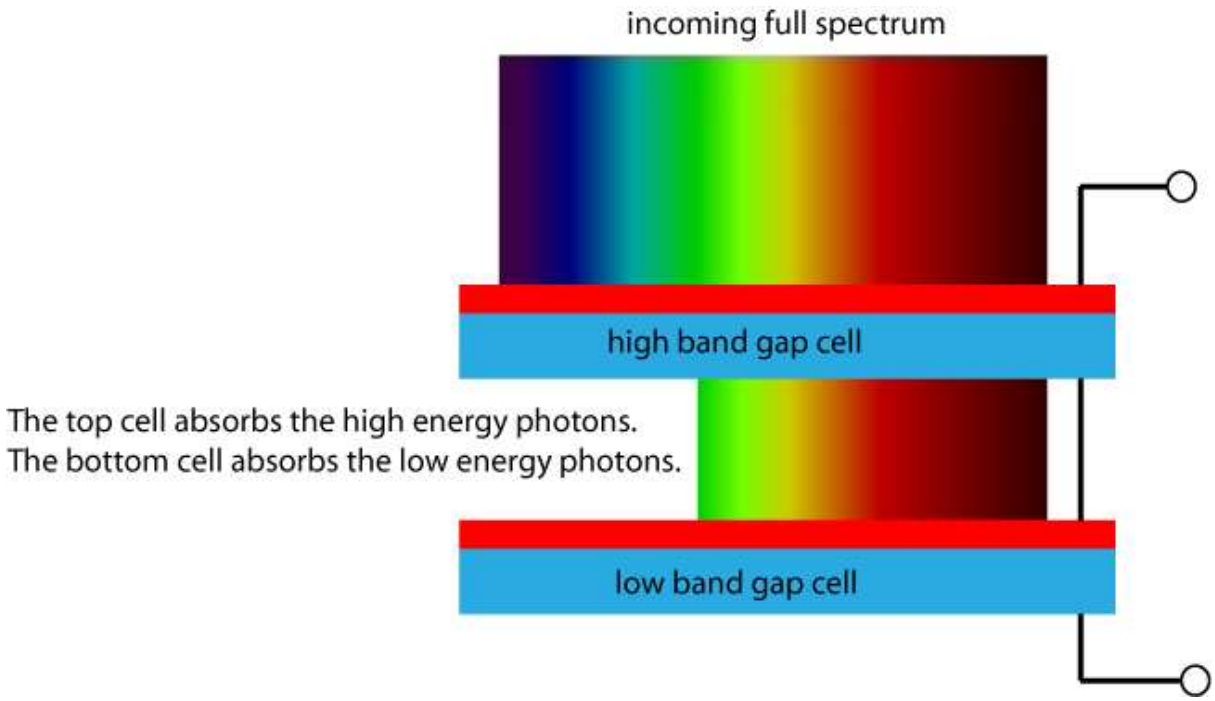


**Fig.9:** Series connected tandem solar cell. Adding more devices allows for each device to be optimized to a narrower spectrum giving a higher overall efficiency.

Tandem solar cells can either be individual cells or connected in series. Series connected cells are simpler to fabricate but the current is the same though each cell so this constrains the band gaps that can be used. The most common arrangement for tandem cells is to grow them monolithically so that all the cells are grown as layers on the on substrate and tunnel junctions connect the individual cells.

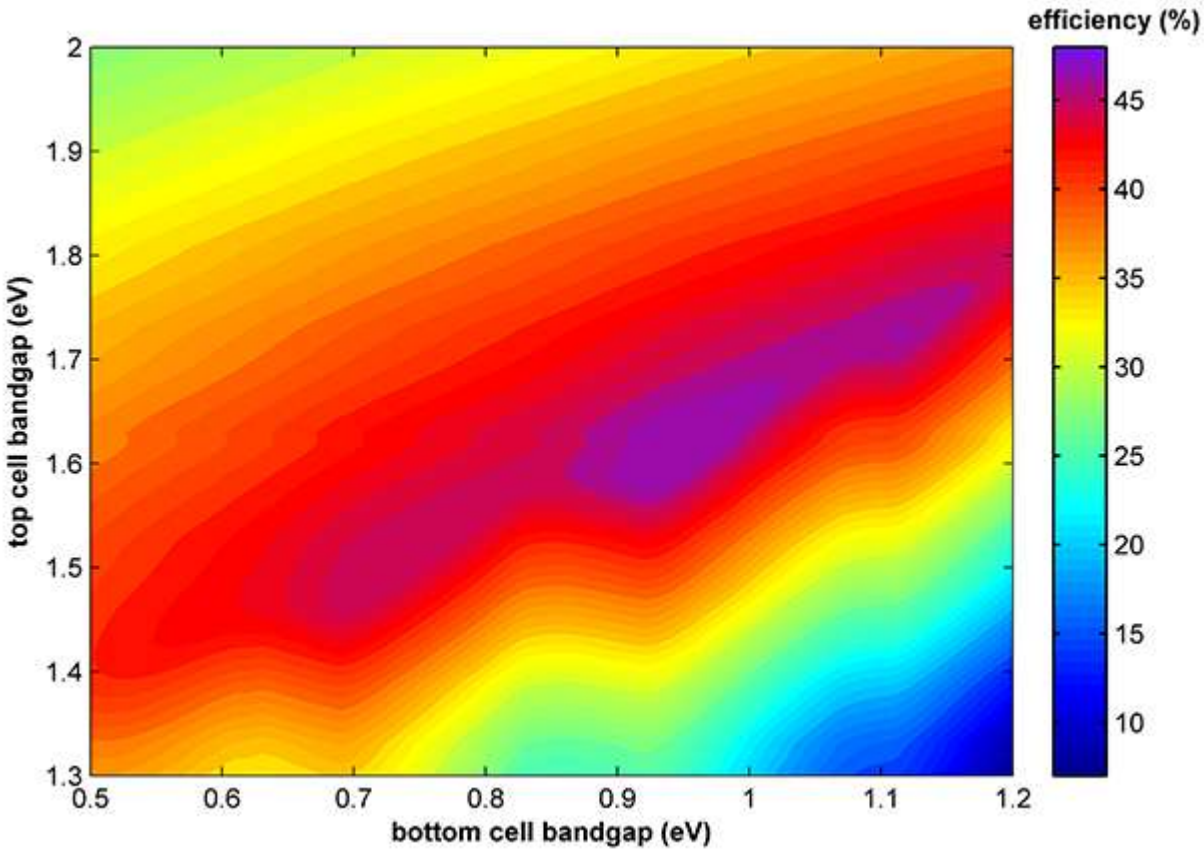


**Fig.10**

The maximum efficiency for a two junction tandem under the AM1.5G spectrum and without concentration is 47 %. At the peak efficiency the top cell has a band gap of 1.63eV and the bottom cell has a band gap of 0.96eV.

As the number of band gaps increase the efficiency of the stack also potentially increases. In reality, the semiconductor materials do not exist to allow for arbitrary materials with a specific band gap and of high quality.

## 1.9 THIN-FILM SOLAR CELL

### 1.9.1 Definition

A type of device that is designed to convert light energy into electrical energy (through the photovoltaic effect) and is composed of micron-thick photon-absorbing material layers deposited over a flexible substrate. Thin-film solar cells were originally introduced in the 1970s by researchers at the Institute of Energy Conversion at the University of Delaware in the United States. The technology continuously improved so that in the early 21st century the global thin-film photovoltaic market was growing at an unprecedented rate and was forecast to continue to grow. Several types of thin-film solar cells are widely used because of their relatively low cost and their efficiency in producing electricity.

### 1.9.2 Types of Thin-Film Solar Cells

Cadmium telluride thin-film solar cells are the most common type available. They are less expensive than the more standard silicon thin-film cells. Cadmium telluride thin-films have a peak recorded efficiency of more than 18 percent (the percentage of photons hitting the surface of the cell that are transformed into an electric current). By 2014 cadmium telluride thin-film technologies had the smallest carbon footprint and quickest payback time of any thin-film solar cell technology on the market (payback time being the time it takes for the solar panel's electricity generation to cover the cost of purchase and installation).

Copper indium gallium selenide (CIGS) is another type of semiconductor used to manufacture thin-film solar cells. CIGS thin-film solar cells have reached 20 percent efficiency in laboratory settings and 14 percent efficiency in the field, making CIGS a leader among alternative cell materials and a promising semiconducting material in thin-film technologies. CIGS cells traditionally have been more costly than other types of cells on the market, and for that reason they are not widely used.

Gallium arsenide (GaAs) thin-film solar cells have reached nearly 30% efficiency in laboratory environments but they are very expensive to manufacture. Cost has been a major factor in limiting the market for GaAs solar cells; their main use has been for spacecraft and satellites.

Amorphous silicon thin-film cells are the oldest and most mature type of thin-film. They are made of non crystalline silicon, unlike typical solar-cell wafers. Amorphous silicon is cheaper to manufacture than crystalline silicon and most other semiconducting materials. Amorphous silicon is also popular because it is abundant, nontoxic, and relatively inexpensive. However, the average efficiency is very low, 10 percent.

### 1.9.3 Application of Thin-Film Solar Cells

Applications of thin-film solar cells began in the 1980s with small strips that were used for calculators and watches. Throughout the early 21st century the potential for thin-film applications increased greatly, because of their flexibility, which facilitates their installation on curved surfaces as well as their use in building-integrated photovoltaic system.

As thin-film solar cells continue to improve in efficiency, it is predicted that they could overtake the classic inflexible photovoltaic technologies that have been in use since the mid-20th century. Sheets of thin-films may be used to generate electricity increasingly in places where other photovoltaic cells cannot be used, such as on curved surfaces on buildings or cars or even on clothing to charge handheld devices. Such uses could help to achieve a sustainable energy future.

## 1.10 SnS (Herzenbergite)

### Basic Info

Tin (II) Sulfide (SnS) is a brown solid and is insoluble in water. Its occurrence in nature takes the form a herzenbergite, which has an orthorhombic crystal structure. SnS also has hexagonal (wurtzite) and cubic (Sphalerite) crystal forms which are less stable than herzenbergite at room temperature.

### Crystal Structure

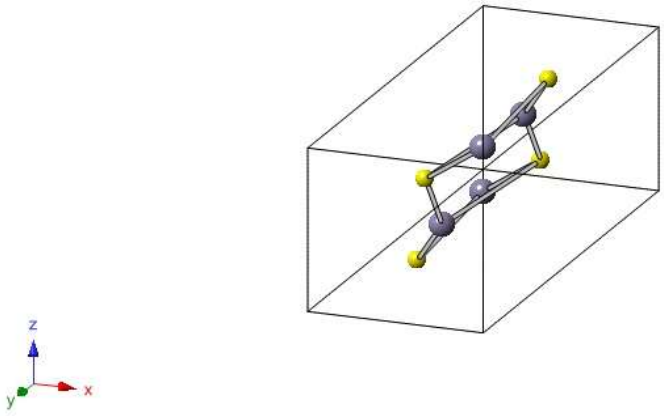


**Fig. 11a**

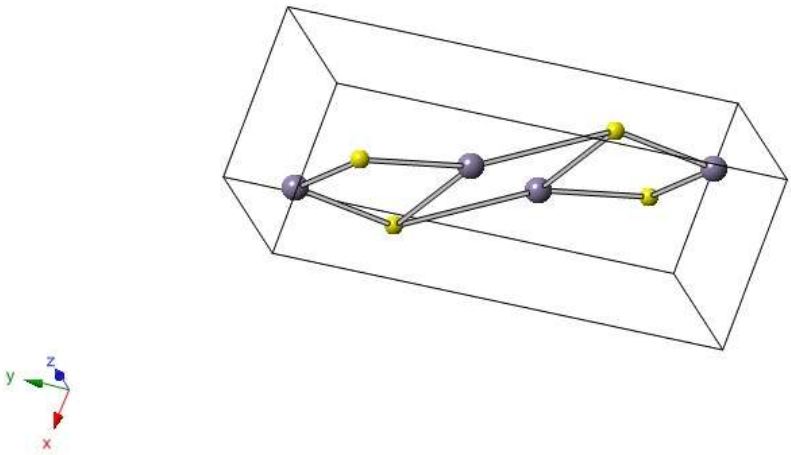


**Fig. 11b**

The graph below shows peak intensities for SnS:

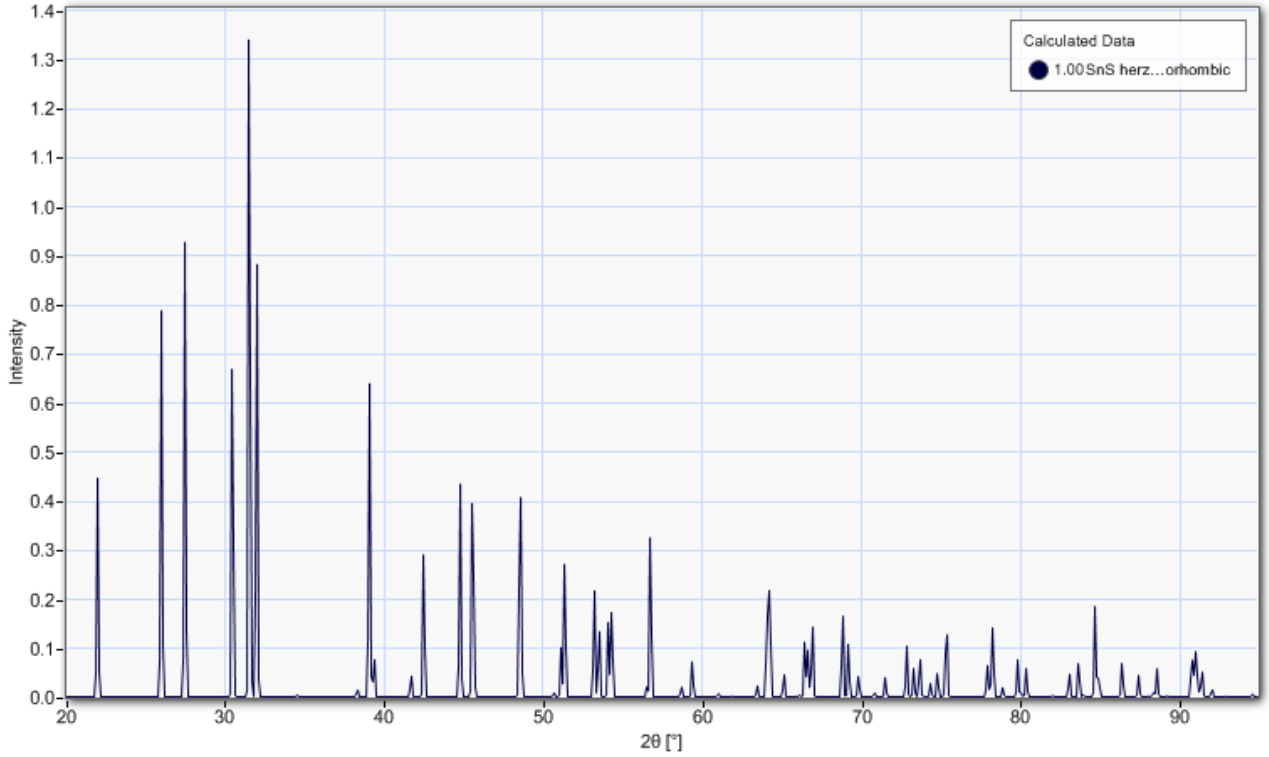


**Fig. 12**

**PV Applications**

SnS is a p-type semiconducting material with a layered orthorhombic structure. It has little toxicity to humans and the environment as well as a band gap of 1.0-1.5 eV.

This makes SnS a suitable option as the absorption layer in n-type solar cells with a wide band gap. Various techniques of fabricating SnS thin films include: vacuum evaporation, chemical bath deposition, and spray pyrolysis.

**Table 1 : Basic Parameters at 300 K**

| | |
|---|---|
| Crystal structure: | Orthorhombic |
| Number of atoms in 1 $cm^3$: | 4.15 x $10^{26}$ |
| Unit cell volume: | 192.6 $Å^3$ |
| Atoms per unit cell: | 4 |
| Debye temperature: | 270 K |
| Density: | 5.08 $g/cm^3$ |
| Lattice constants: | |
| | a= 4.33 Å |
| | b = 11.18 Å |
| | c = 3.98 Å |

## 1.11 Current status of PV conversion system

The sphere of Solar Cells science has been dominated by the devices comprising junction of between solid state materials, usually doped forms of crystalline or amorphous Si and making profit over the experience and material availability resulting from semiconductor Industries.

But for cost effective Solar Cells, global efforts have been made by R &D to harvest reduction in consumption of Si and other materials as well as with improved efficiency. These efforts paved the foundation path for thin films and scientists get included to thrive for absorbent layers other than available ones such as Hetero junction. The thin film like $CuInSe_2$ (CIS), were studied over decades and decades. Modules so manufactured with thin films efficiency nearly 12% but the major concern was about the toxicity of Cadmium and the prior degradation in exposure to domestic environment besides numerous efforts these disadvantages were not yet swiped. Contemporary efforts are to develop new PV materials to improve efficiency without these demerits.

The factors taken into account in developing new PV materials include:-

i) A suitable energy band gap.
ii) Low cost deposition.
iii) Material availability in abandoned its accessibility.
iv) Pollution free disposal of modules.

It' s been long time that continuous efforts has been given to find out the most appropriate material to be used as absorber material for Solar Cell and some advanced material has been proposed to as potential absorber material still some disadvantages remain like non-availability, toxicity, durability, reproducibility are yet to be cleared out.

## 1.12 Objective of the Present Work

The foremost challenges confronting the researchers regarding the contemporary energy crisis are to obtain cheap and efficient solar cells. So rigorous attempts has been made to hunt quality based thin films instead of involving in bulky materials.sns owes the position of excellent absorption material in thin film solar cells. However, numerous efforts were made to fabricate a high quality crystalline SnS thin film through different methods.

Successive ionic layer adsorption and reaction (SILAR) is completely newer and improved version of chemical bath deposition (CBD) method which can deposit large area thin film without any external source of energy. But deposition relies on many chemical and physical factors which are needed to be optimized to rectify the backlash errors so as to tune the band gap of thin film so obtained. To overcome the above obstacles, this work is dedicated for optimisation with varying concentration of anionic precursor as well as to determine other instrumental factors to get a crystalline structure. Besides these to find out the structure and composition of different phases of Stannous sulphide and dominant phases among them in different samples with help of SEM IMAGES,EDX,XRD.

## 1.13 Scope of the Present Work

The present work has been presented with clear motive to sensitize the economically cheap fabrication of $Sn_XS_Y$ through SILAR process in a judicious sequence of optimization to tune its band gap and channelize it to the main stream of commercialization of solar cell technology.

The entire work comprises of three steps:-

1) Fabrication of SnS thin film with three different concentration of anionic precursor keeping constant the cationic precursor.

2) Qualitative and quantitative analysis of thin film.

3) Structural analysis of thin films.

The entire work is presented as a thesis containing six chapters. First chapter deals elaborately with the introduction and working principle of solar cell, thin films and aims and objective of the work. The study of related journal papers has been presented in the second chapter. The

third one comprises the fabrication of $Sn_XS_Y$ films through SILAR process. the fourth one simply represents a brief introduction of XRD, SEM and EDX. The results so obtained after the tests (SEM, EDX, XRD) and the discussion on the results along with the conclusion are included in the fifth chapters. The sixth and the last chapter includes summary of the work wherein we have discussed the work along with the results and added concluding remarks which explains that defects and mistakes committed in our work and the precaution to avoid such mistakes.

There can be many other ways of optimization but as the process lays down on numerous constraints at the preliminary stages of fabrication which have a noteworthy affects on the crystal structure of the thin films. Our aim is to start with judicious sequence to extract best even from grass root level then move to further higher methods like annealing and doping etc. to procure such a quality of SnS thin films which guaranties to meet the global needs and can withstand the global challenges.

# 2. REVIEW OF THE PREVIOUS WORK

## 2.1 Introduction

Nowadays, a fabrication of low-cost, environmentally benign and highly efficient photo-electrochemical (PEC) energy conversion devices for empowering the variety of electronic appliances is one of the great challenges for the researchers worldwide [42-45]. The considerable attention has been paid on the preparation and development of key materials, as the performance of these devices relays on the properties of materials [46]. As compared to the bulk materials, thin films possess periodicity at most in two-dimensions, causing the enormous variation in its physio-chemical properties than that of bulk materials.

Thin film technology has wide range of applications in various areas. It is a base of outstanding developments in the various fields of science and technology such as solid-state electronics, optics, magnetism, coatings, super capacitor and photovoltaic (PV) cells. The advantages of thin film devices over the bulk materials are low material consumption, easy processing and possible use of flexible substrates [47]. It is well known that the properties of thin films are dependent on the method of deposition. The required properties and flexibility can be achieved by choosing the appropriate deposition method for thin films. Thin film deposition methods can be broadly classified into physical and chemical methods. In physical methods, vacuum evaporation and sputtering are enclosed, in which material to be deposited is transferred to a gaseous state either by evaporation or an impact process and deposited on the substrate [48]**.** The chemical methods include the gas phase chemical processes such as conventional chemical vapour deposition (CVD), laser CVD, photo CVD, metal-organic CVD (MOCVD), electro-deposition (ED), chemical bath deposition. (CBD), modified chemical bath deposition (M-CBD), successive ionic layer adsorption and reaction (SILAR), spray pyrolysis, sol-gel, etc. The chemical methods unified with growth from chemical solution. The physical methods have major drawbacks such as high working pressure, requirement of sophisticated equipments, high cost, cleaning after each deposition etc., Chemical methods are simple, economic and convenient for the deposition of variety of materials such as metal chalcogenides, metal oxides, metal hydroxides and materials with complex chemical compositions in the thin film form [8, 9]. The broad classification of thin film deposition methods is mentioned in 2.2.

Among these thin film deposition methods, successive ionic layer adsorption and reaction (SILAR) method is relatively simple and offers wide range of advantages over other expensive methods of thin film deposition [10-12] such as

1. It is a process in which the deposition rate and thickness of the film can be easily controlled over a wide range by changing the deposition cycles.
2. Relatively uniform films can be obtained on substrates of any shape; there is no restriction on substrate material, dimensions or its surface profile.
3. Unlike vacuum based deposition method, SILAR method does not require any expensive and sophisticated instruments and also vacuum at any stage which is a great advantage in the context of an industrial application.
4. The SILAR method usually requires low operating temperature. Apart from the obvious advantages in terms of energy saving, low deposition temperature avoids high temperature effects involved in different processes such as inter diffusion, contamination and dopant redistribution.

## 2.2 Thin Film Deposition Methods

Thin film deposition methods are broadly classified into :-

a)Physical methods and b)Chemical methods

Physical methods are further subdivided into:-

i)Vaccum methods –Relative heating , Flash evaporation ,Electron beam evaporation,Laser evaporation ,Arc evaporation and Radio frequency (RF) heating.

ii) Sputtering methods–Glow discharge, DC Sputtering, Triode Sputtering, Getter Sputtering, Radio frequency (RF) Sputtering, Magnetron Sputtering, Ion beam Sputtering, AC Sputtering.

Chemical methods are further subdivided into:-

ii)Gas phase–Chemical vapour deposition(CVD),Laser CVD,Photo chemical vapour deposition,Plasma enhanced CVD,Metal organochemical vapour deposition.

ii)Liquid phase–Electrodeposition,Electroless deposition,Spray pyrolysis,Chemical bath deposition,SILAR(Successive ion layer adsorption and reaction) deposition.

### 2.3 SnS as a photovoltaic material (Salient features)

SnS (Tin Sulphide) is a p-type semiconducting material with band gap 1 – 1.5eV and little toxic to human and environment.

SnS is a IV – VI compound that has recently become interest for application as absorber layer in cost effective thin film Solar Cell. Unlike CdTe and CIGS, It has optimum energy band gap for PV solar conversion and high and high optical absorption coefficient for photons with energies greater than its band gap such that few microns of material are needed to absorb most of the incident light thus minimizing the material consumption and cost. At room temperature, SnS exhibits stable, low symmetric, double layered orthorhombic crystal structure, having a=0.4329, b=1.1192 and c=0.3984nm as lattice parameters.

These layered structure materials are of interest in various device applications due to arrangements the structural lattice with cations and anions. The layers of cations are separated only by Van der waals forces that provide intrinsically chemically inert surface without dangling bonds and surface density of states. This also leads to considerably high chemical and environmental suitability. Besides, electrical and optical properties of SnS can be replenished by rectifying the growth condition by introducing complex agent or post deposition -- or doping etc.

Tin forms –binary components with sulphur namely- SnS (orthorhombic), $Su_2S_3$ (orthorhombic), $Sn_3S_4$(tetragonal),$Sn_4S_5$ etc. of which SnS, $SnS_2$ and $SnS_3$ are of discrete phases. All the binary compounds behave like semiconductor and exhibits p-type or n-type conduction depending upon the concentration of Tin.

**$SnS_2$:** Tin disulphide adopts $PbI_2$layerd structure with hexagonal unit cell, in which tin atoms are located in the –sites between the two hexagonally cloud pack sulphur slabs to form sandwich structure. It is normally n-type and band gap is in the range of 2.12 – 2.44eV.

**$Sn_2S_3$:** It is classified as a mixed valence compound which exhibits n-type conductivity having band gap 0.95-1.16eV and whose optoelectronic properties on its crystalline structure and stoichiometry.

## 2.4 Objectives of fabrication of Tin sulphide

Tin sulphide films can be obtained by physical as well as chemical methods. For different methods the following crucial factors should be taken into consideration while depositing.

1. Dominant phase- It is different to obtain single phase of SnS with no or traces of $SnS_2$ present. Thus it is the aim to depth which depends in the mixture.
2. Crystal quality – The diffusion length must be long compared to the absorption depth which depends in crystal quality.
3. Low Cost – Deposition method should be cost effective.
4. Low toxicity – Deposition method and end products should not be toxic and can be easily disposed.
5. Grain size – Grain size should be large enough for high conductivity.

## 2.5 Review of previous works

S. Sohila. et.al [1] has prepared SnS nanosheets by wet chemical route using ethylene glycol (EG) and without any surfactant. Morphology and particle size were confirmed under TEM (Transmission electron microscope) and HRTEM (High Resolution).

Phase purity is confined using X-ray diffraction technique and found only one highest peak of <111>plane which implies orthorhombic structure of SnS. UV-VIS-NIR absorption spectrum shows the direct band gap of 1.88 eV compared to bulk band gap. It has undergone a blue shift of 0.58 eV. At room temperature photoluminescence spectrum shows two emission band gap at 1.75 and 1.57eV which can be removed by annealing. $SnCl_2.2H_2O$ as source of Sn and $Na_2S$ as source of sulphur and EG as solvent is used. Stoichiometric ratio of 1:3 $SnCl_2.2H_2O$ and $Na_2S$ were used for precipitation at 80 $^0$C through drop by drop addition of $SnCl_2.2H_2O$ in $Na_2S$. The dark brown colour indicates the formation of product.

Different values of energy gap have been obtained for SnS ranging from 1 to 2.33eV depending on the resulting structure obtained by different techniques and the occurring type of electron transitions. The requirements imposed on films used as a light absorber are (i) they must have an energy gap of about 1.5eV with indirect allowed transition and (ii) a high absorption coefficient >104 $cm^{-1}$. Because SnS crystallizes in orthorhombic structure, it can be used in n–p homo-junction and n–p hetero junction. SnS thin films can be prepared by a variety of methods with the purpose of manufacturing thin films suitable for use as a solar absorber in optoelectronic devices and photovoltaic applications. M.M. El- Nahass et.al [2] has shown that thermally evaporated SnS amorphous films undergo structural transformation upon annealing in the temperature range between 432K–573 K. SnS is the only structural phase grown during annealing of SnS film in the range 373-573K. A significant growth of <101> and <111> plane when annealed at 473K and resulted in energy gap of 1.38eV and absorption coefficient >105 $cm^{-1}$. Annealed and non annealed SnS thin films are transparent >1250nm and dispersion energy Ed are 3.85eV and 20.25eV respective. The type of optical transition responsible for optical absorption are indirect allowed or direct-forbidden transitions with energy gaps of 1.4 and2.18 eV for amorphous films and of 1.38 and 2.33eV for crystalline films.

Arindam Basak et.al [3] proposed a work observing effect of substrate on the properties of SnS thin film grown by thermal evaporation method. They found that SnS thin films were grown on different substrates glass/ ZnO: Al, glass/ITO, and glass CdS by thermal evaporation

method. XRD pattern shows that all the films so deposited shows <111> primitive orthorhombic structure. Out of three films with glass/ZnO Al shown better crystallinity and less dislocation density. EDAX analysis shows that film with substrate glass/ITO shows nearly empirical ratio of 1:1 but the majority of metal ions creates accepter states turning them all as p–type with activation energy 0.22eV to 0.45eV. Optical characteristics of three samples are observed under light of wavelength 800-900 nm. They have showed a right shift in transmittance with decreasing inter planar distance.

SEM (scanning Electron Microscope) shows film glass/ZnO:Al has densely packed grains whereas island and flake type structures are found with cracks also due to increase in dislocation density. Hall effect shows that all are p-type with mobility and conductivity being highest in glass/ ZnO: Al substrate due to packed regular grain. I-V characteristics implies that contact ZnO:Al/SnS is rectifying rather than ohmic because work function of ZnO:Al ($\phi$= 3.99eV) less than work function of SnS ($\phi_s$=4.2eV) but in case of ITO, it is reversed.

Arindam Basak et.al [4] proposed a paper work in which they have detailed the impact of substrate temperature by deposition SnS thin films on soda lime glass at three different temperatures using thermal evaporation method. SEM images shows worm like structure with voids below room temperature and 300 °C but at 450 °C these grain became packed with granular structure. EDAX shows Sn:S ratio first decreases then increases but at high temperature desulphurization occurs. XRD data shows orthorhombic structure with highest peak for <110> plane at 300 °C, they observed best crystallinity. Transmittance decreases with the increase of temp. It may be due to small losses of sulphur with increasing temperature. There is reduction of band gap but at high substrate temp. $E_g$ is not affected. Refractive Index and dielectric strength shifts toward longer wavelength with increase in substrate temperature as well as both quantities decreased in magnitude also. Extinction coefficient determines how strongly a substrate can absorb light. Extinction coefficient Vs wavelength graph shows no major variation with substrate temperature. With the increase in substrate temperature mobility of carriers increases and resistivity decreases. The carrier concentration range lies within $10^{14}$.

The structural and optoelectronic properties of vacuum evaporated SnS thin film annealed in argon ambient has been studied by Biswajit Ghosh et.al [5]. The 650nm polycrystalline SnS thin Film were grown by thermal evaporation of high purity tin sulfide powder at 250 $^0$C substrate temperature, followed by post deposition annealing process is carried out at 200 °C and 300 °C for 2h, 4h & 6h and 400 °C for 2h and 4h. XRD pattern of SnS thin film confirmed

orthorhombic polycrystalline structure with predetermined peaks of <101>, <111>, <131> with peaks <111>&<421> showing Sn2S3as a slight impurity. SEM images confirmed worm like grains in irregular order with void with annealing dislocation density deceases. EDAX study shows that Sn/S ratio decreases with increasing temperature of annealing and there is slight desulphurisation at high temperature annealing at 400 °C. Initially, the films show low transmittance in visible range due to interference fringe. At high temperature annealing for longer duration 400 °C for 2h or 4h ).

The interference fringes disappear and transmittance curves were smooth. Band gap $E_g$ decreases with increase in annealing temperature and duration of shows a radiation of 1.53 – 1.33eV. Similarly bulk resistivity varies from 127 – 83.2 Ω-cm. Carrier concentration unit volume increases annealing temperature and duration due to absence of voids.

N. Koteeswara Reddy et.al [6] presented a paper in which they have studied the electrical properties variation with substrate temperature in spray pyrolytic sulphide films. It has been reported that films formed at substrate temperature below 200 °C. The film grown with substrate temperature $T_s$<300 °C and $T_s$>375 °C are n-type and for 300 °C <$T_s$< 375 °C are p-type. It might be due to variation of stoichiometry of films with Ts. The excess sulphur at low temperature and presence of oxygen at high temperature is the cause of getting n-type films. Resistivity decreases with the increase of substrate temperature showing almost constant ρ of 300 Ω-cm in the substrate temp range of 300 °C – 375 °C. It has been observed that carrier density ad Hall mobility increases with the increases with the increase in temperature.

Thin film of tin (II) sulfide was prepared by the spray pyrolysis technique using aqueous solution of as received $SnCl_2$ (SC) (>99% from Sigma Aldrich) and Thiourea (TU) (>99% from Sigma Aldrich). Malkesh kumar Patel et.al [7] presented this paper to highlight the effect of molar concentration on the structural, morphological, optical and optoelectronic properties of SnS thin film on F: SnO2 coated glass substrate. XRD pattern shows dominant peak <111> plane was more intense as molar ratio $SnCl_2/Na_2S_2O_3$ (thiourea) was varied from 1/1-1/1.3. Microstructure analysis shows that deposited film have uniform and having surface free from cracks pinholes. The comparison of film was maximum for ratio of 1/1.3 and 1/1.45. In comparison of as deposited film this S concentration was found to increase linearly as the major concentration ratio of SnCl2/Na2S2O3 varied from 1/1 to 1/2. Reporting band gap 1.7 – 1.78eV, $\alpha = 1.42 – 2.85 \times 10^7$ $cm^{-1}$ with varying thickness and optimum molar concentration ratio of 1/1.3 generating a photocurrent of 0.4 mA $cm^{-2}$.

T.H. Sajeesh et.al [8] obtained that when Ts was in range of 300-400 °C, all the surface were uniform free of pinholes and crack with brownish colour at Ts = 375 °C. They got stoichiometric SnS films at Ts>450 °C desulphurization occurs. Film prepared with 300 °C<Ts<400 °C were of p-type SnS phase and with Ts>450 °C were of $SnS_2$ phase and of n-type. Therefore Ts = 375 °C was chosen for further deposition of SnS films. Optimisation of precursor ratio for p-type absorber layer can be done. They got 0.2 M of Ms at 375 °C resulted in the formation films with SnS phase, with Ms>0.2M shows SnS2 phase and Ms<0.2 M showed presence of the 'mixed valency' compound $Sn_2S_3$. Its Optimisation of n-type absorber layer can be done by regulating the concentration of Sn. High sensitivity of 2.3 is recorded for $M_{sh}$= 0.06M. Resistivity decreases upto Msh = 0.1M and then increases slightly may be due to type conversion.

High quality of single phase SnS and suitable device structure with proper band alignment between different junction materials are required in order to achieve high efficiency SnS solar cell. The different elemental compositions of tin and sulfur can form several binary compounds such as SnS, $SnS_2$, $Sn_2S_3$, $Sn_3S_4$, $Sn_4S_5$. The co-existence of different phases in the tin sulfide film influences the electrical and optical characteristics of the photo-absorber. Tin monosulfide (SnS) is p-type material whereas $SnS_2$ and $Sn_2S_3$ are n-type materials. Therefore, small change in composition could result in type inversion of conductivity. Tanka Raj Rana et.al [9] observed the annealing imposes the crystallinity film deposited by rf sputtering method, XRD and Raman spectroscopy shows as deposited film contain α–SnS and π-SnS with $SnS_2$ and $Sn_2S_3$ phase which get converted into α-SnS. The optical band gaps of as deposited and post annealed films are 1.46 eV and 1.25 eV repectively. So, the multiple phase defects are the most crucial factors for lower efficiency of SnS film.

Malkeshkumar Patel et.al [10] have studied the effect of annealing over structural and optical properties of sprayed SnS thin film XRD pattern shows SnS2 as a secondary phase in all sprayed thin SnS film, however a large properties of SnS phase was found to grow at higher annealing temperature making the film SnS2 deficient. Annealing at 500 °C, the film shows pure phase of Sns with <111> orientation. SEM images shows that films become denser at higher annealing temperature along with the improvement of roughness factor. Due to densification absorption factor increases as well as $E_g$ shows an increment not to an observable extent. The sprayed SnS thin films could be become more degenerate and less resistive by

annealing treatment. They recommended to optimize post annealing condition for spray deposited SnS to have best superior quality of optical characteristics.

There are recent reports on post-deposition annealing of SnS thin films and its effect on film stoichiometry and formation of secondary phases. In the case of films grown by vacuum thermal evaporationat250 $^0$C, it was observed that the film is relatively tolerant to annealing at temperature of 300 $^0$C; however, higher annealing temperature has resulted in the segregation of Sn phase. N.R. Mathews et.al [11] observed that in pulse electrodeposited SnS thin films there is formation of $SnS_2$ phase at annealing temperature >350 °C which leads to increase in band gap of 0.1 eV and resulted in decrease of photosensitivity. They concluded in case of deposition technique, high temperature annealing leads to instability of SnS films with trap levels of 0.1 eV, 0.05 eV, 0.03eV.

SnS could have been deposited using a variety of techniques including spray pyrolysis, electrodeposition, chemical bath depositionand vacuum evaporation. The chemical and physical properties of the layers deposited using thermal is evaporation varied with the deposition conditions, including substrate and source temperatures and film thickness. Ogah E. Ogah et.al [12] proposed a paper in which thermally evaporated SnS thin film onto glass and CdS/ITO coated glass annealed in vaccum for optimising them for use in PV solar cell application. The resistivity of annealed layer increased with the increase in substrate temperature and decreases with the increase in source temperature. The annealing enhance the crystallinity, absorption factor and phase purity.

U. Chalapathi et.al [13] observed that in a chemically deposited SnS thin film at annealing temperature of 300 °C for 60 mins, SnS2 peak becomes dominant and the dominance increases with increase in annealing temperature and time.

SEM images shows that short annealing time below 30mins and annealing temperature below 250 °C leads to increase in grain size and improves the crystallinity.

Film annealed with 250 °C for 10mins shows maximum hole mobility and resistivity of 1.03 x $10^{13}$ with average carrier concentration and lowest resistivity among all the specimen.

Biswajit Ghosh et. al [14] observed with XRD that SnS films so deposited has orthorhombic and polycrystalline structure. Both annealed and non-annealed shows peak of <111> plane. But

annealing at 150 °C shows a growth of other peaks like <101>, <141>, <002> which are eliminated on further annealing.

In-SnS-In films show ohmic behavior in all annealed condition. The I-V characteristics of as deposited and each annealed specimen were not reproducible. It is seen that the contact has short key type behavior and resistivity increases with increase in annealed temperature.

Ag-Sn-In specimen also shows shottky type behaviour only in as deposited form.

Al-Sn-In specimen with increase in annealing temperature the barrier height decreases and at 350 °C of annealing shows ohmic behavior. But with the annealing temperature, the break down voltage of metal semiconductor interface decreases.

B. Ghosh et.al [15] carried out the process of basic through four basic steps.

a) low resistivity and high transmittive CdS film preparation
b) fabrication of SnS layer onto CdS.
c) SnS/CdS junction formation.
d) back contact formation.

Here SnS is p-type and CdS is n-type laid down over ITO layer deposited on glass substrate.

XRD shows that there exists only SnS phase and the junction is characterized with high series resistance due to small grain size of SnS layer which leads to low efficiency.

They have focused on enhancement of grain size of window layer (CdS) only. with $CdCl_2$ treatment. There was no effect on the grain size but it has led to the increase in Isc and Voc of the junction. It may be in also due to post deposition heat treatment of SnS layer and etching of CdS. The author recommendations for enhancement of efficiency are :-

a) Etching of CdS window layer
b) Post annealing of absorber SnS layer for large grain size.
c) Lattice matching window layer.
d) Optimisation of thickness of window and absorber layer.

S. Das et.al [16] $Cu_2S$ thin films of well-controlled thickness and stoichiometry were prepared by a solid state reaction between CdS and CuC1 films in the temperature range 200-250 °C. The $Cu_2S$ films exist in the orthorhombic chalcocite phase. The growth of $Cu_2S$ on CdS is topotactial, and the chalcocite phase is obtained on reaction with both wurtzite and sphalerite structures of CdS. The electrical and optical properties of the $Cu_2S$ films are consistent with the $Cu_2S$ composition. These films were utilized to fabricate $Cu_2S$/CdS solar cells.

Khaldun A. Salman et al [17] Two texturing methods using porous silicon (PS) and pyramids were performed to investigate the effect of them on the performance of crystalline silicon (c-Si) solar cell. Surface morphology and structural properties of samples have been studied using scanning electron microscopy (SEM) and atomic forces microscopy (AFM). Optical reflectance was obtained using optical reflectometer. I-V characterization of fabricated solar cells was investigated. The results showed the highest conversion efficiency of 13.23% for PS layer compared with 11.36% and 3.70% efficiencies for the solar cells devices with pyramids texturing

and as-grown Si, respectively. PS texturing exhibited an excellent reduction in the reflection of incident light compared with pyramids texturing process, with a good light-trapping of wide wavelength spectrum, which could produce high efficiency solar cells.

Metin Kul et.al [18] SnS film has been produced by electro deposition technique onto ITO (indium-tin-oxide) coated glass substrates using aqueous solution containing $SnCl_2$ and Na2S2O3. The pH of the solution was adjusted to 1.8 by drop-wise addition of 0.1 M HCl before the deposition. The SnS films were electrodeposited at constant potential value (1.0 V relative to the saturated calomel electrode) in this study. The electro deposition was carried out at 20°C under constant stirring at 60 rpm in the bath. The deposition time was 30 min. The deposited film was uniform, well adherent and dark brown in colour .The SnS film has been characterized by X-ray diffraction (XRD) and Fourier transform infrared (FTIR). The sample is polycrystalline in nature with orthorhombic phase having (101) and (040) preferential orientations. The crystallite size, texture coefficient, lattice parameters, strain and dislocation density were estimated from XRD results. Surface morphological studies were carried out by using Field Emission Scanning Electron Microscopy (FESEM). The band gap of the SnS film has been studied using the optical absorbance measurement as a function of wavelength between 200 and 3000 nm. The direct band gap of the sample is calculated to be 1.1 Ev. The conductivity type of the sample was determined as p-type by using the Hall effect

measurement. The Hall mobility of the sample had also been measured with temperature by means of the Hall effect.

A Arulanantham et.al [19] Herein we report a well-organized analysis on various key-properties of SnS thin films for solar cell fabricated by nebulizer spray pyrolysis technique. X-ray diffraction study reveals the polycrystalline nature of deposited films with orthorhombic crystal structure. The crystallite size was calculated and observed to be in the range of 8e28 nm with increasing molarity of precursor solution. The stoichiometry composition of SnS was confirmed by EDX study. SEM/AFM studies divulge the well-covered deposited surface with spherical grains and the size of grains is increasing with concentration and so the roughness. A remarkable decrease in band gap from 2.6eV to 1.6eV was noticed by raising the molar concentration from 0.025 M up to 0.075 M. A single strong emission peak at about 825 nm is observed in PL spectra with enhanced intensity which may be attributed to near band edge emission. From the Hall effect measurement, it was found that the SnS thin film exhibits p-type conductivity. The calculated values of resistivity and carrier concentration are 0.729 Ω-cm and 3.67 - 1018/cm3 respectively. Furthermore, to study the photovoltaic properties of SnS thin films a hetero junction solar cell, FTO/n-CdS/p-SnS was produced and the conversion efficiency was recorded about 0.01%.

N. Koteeswara Reddy et.al [20] The contact behavior of tin monosulfide (SnS) nanocrystalline thin films with zinc (Zn) and silver (Ag) contacts was studied. SnS films have been deposited on glass substrates by thermal evaporation technique at a growth temperature of 300 °C. The as-grown SnS films composed of vertically aligned nanocrystallites with a preferential orientation along the b010N direction. SnS films exhibited excellent chemical stoichiometry and direct optical band gap of 1.96eV. These films also exhibited excellent Ohmic characteristics and low electrical resistivity with Zn contacts. The observed electrical resistivity of SnS films with Zn contacts is 22 times lower than that of the resistivity with Ag contacts. The interfacing analysis reveals the formation of conductive Zn–S layer between SnS and Zn as interfacial layer.

Kosuke O. Hara et.al [21] Metastable cubic SnS phase (*p*-SnS) is an emerging material having attractive properties for solar cell applications. In this study, we have investigated the thermal evaporation process of SnS with substrate temperatures of 250–350◦C, and have observed the formation of *p*-SnS together with the stable orthorhombic phase (*a*-SnS) for the first time by using only SnS as a starting material. X-ray diffraction analysis shows that a single-phase *a*-

SnS film is obtained at 350°C, and the fraction of *p*-SnS increases with decreasing the substrate temperature to 250°C. The grain shape of the SnS film grown at 250°C observed by scanning electron microscopy was more isotropic than 350○°C, consistent with the cubic lattice of *p*-SnS. Electrical characterization by Hall measurement reveals the existence of the maximum point of carrier density as a function of substrate temperature, which is understood by the competition between the increases of crystal defects and the fraction of wider-gap *p*-SnS than *a*-SnS with decreasing substrate temperature. The formation of *p*-SnS brings about lowering of absorption coefficients below the absorption edge of *p*-SnS, which are analyzed from transmittance and reflectance spectra. The reason of *p*-SnS formation is discussed by comparing the conditions of film deposition with previous reports.

F. Guo et.al [22] SnS films with different Sn contents were fabricated by thermal co-evaporation. The variation in structures, optical and electrical properties of SnS with different Sn contents was systematically investigated. The prepared films were characterized by X-ray diffraction, field emission scanning electron microscopy, and energy dispersive spectroscopy analysis. An excess of Sn can result in a change of the SnS semiconducting film from p-type to n-type. The SnS films showed band gaps in the range of 1.25–1.57eV and high mobility of 7.29 $cm^2/V{\cdot}s$, indicating suitability for application in photovoltaic cells. The photoelectric conversion efficiency (PCE) of the hetero junction solar cell was 1.26% with a open circuit voltage (VOC) of 0.153 V and a short circuit current density (JSC) of 29.61mA/$cm^2$.

Jacob A et.al [23] Tin mono-sulfide (SnS) is a promising Cd-free candidate as absorber layer in Thin Film Solar Cell technology. In this work SnS thin films were synthesized by chemical spray pyrolysis (CSP) technique using a 0.2 M equimolar precursor solution of tin chloride and thiourea at substrate temperatures of 350, 370and 390◦C and pressure for 0.5 and 1.0 kg-f/$cm^2$. Characterization of synthesized films was performed by X-ray diffraction, Raman spectroscopy, scanning electron and atomic force microscopy, transmission, reflection and absorption measurements, and electric characterization techniques. Films show an orthorhombic phase, p-type conductivity, a direct optical energy band gap of 1.3–1.7eV and a high absorption coefficient (≥104/cm). In this work, we have found that the in-situ variation of the carrier gas pressure induced n-type electrical conductivity on SnS films, which will allow an in-situ serial fabrication of the SnS homo-junction without the need of additional doping materials.

B. Ghosh et.al [24] CdTe and the associated materials are suffering from ohmic contacting problem due to their high electron affinity and consequently large function. Ni, Au, Pt and Pd have large work function and have possibility to match with CdTe. However, except Ni other materials have problems in large-scale applications. In the present paper possibility of Ni has been explored through work function engineering. Work function and bulk resistivity of Ni has been modulated with other materials like, Cu, Au, Mo, Wand Co. A theoretical model has been developed to calculate the effective work function and bulk resistivity after modulation. Modulated materials have been deposited over thin film CdTe using electroless technique to evaluate the validity between the theoretical and experimental results. Results indicated about good matching between them. To the best of knowledge this is the first time applications on such type of methodology has presented in contact applications to CdTe.

Lili Sun et.al [25] The electronic, magnetic and optical properties of Zn-doped monolayer $SnS_2$have been theoretically investigated with the density functional theory. Numerical results reveal that monolayer $SnS_2$can be easily synthesized by cleaving its bulk crystal. Besides the Zn doping in monolayer $SnS_2$ is energetically favoured under the S-rich with respect to the Sn-rich condition. The doped system exhibits the magnetic ground states due to the formation of defect states above the Fermi level, which are introduced by the hybridization between S-3p states and a small amount of Sn-4d states. The room temperature ferromagnetism can also be realized in Zn-doped monolayer $SnS_2$. The injection of Zn can enhance the absorption efficiency of solar spectrum, especially in the near-infrared light region. Moreover, the Zn doping can enhance the photo-catalytic activity for both the oxygen and hydrogen evolution reactions in the monolayer $SnS_2$.

S.S. Hegde et.al [26] Tin sulfide (SnS) is a material of interest for use as an absorber in low cost solar cells. Single crystals of SnS were grown by the physical vapor deposition technique. The grown crystals were characterized to evaluate the composition, structure, morphology, electrical and optical properties using appropriate techniques. The composition analysis indicated that the crystals were nearly stoichiometric with Sn-to-S atomic percent ratio of 1.02. Study of their morphology revealed the layered type growth mechanism with low surface roughness. The grown crystals had orthorhombic structure with (040) orientation. They exhibited an indirect optical band gap of 1.06eV and direct band gap of 1.21eV with high absorption coefficient (up to $10^3 cm^{-1}$) above the fundamental absorption edge. The grown crystals were of p-type with an electrical resistivity of 120 Ω- cm and carrier concentration

$1.52x10^{15}cm^{-3}$. Analysis of optical absorption and diffuse reflectance spectra showed the presence of a wide absorption band in the wave length range 300–1200nm, which closely matches with a significant part of solar radiation spectrum. The obtained results were discussed to assess the suitability of the SnS crystal for the fabrication of optoelectronic devices.

M.M. El-Nahass et.al [27] Thermally evaporated SnS amorphous chalcogenide films undergo structural transformation upon annealing in the temperature range between 432K–573 K. The optical properties of amorphous and annealed films were investigated using spectro-photometric measurements of the transmittance and reflectance at normal incidence in the wavelength range 250–2500 nm. The films are transparent for a wavelength >1250 nm. The refractive index (n) and the absorption index (k) are independent of film thickness in the measured film thickness range (55–365 nm). The dispersion energy, $E_d$, of amorphous films increased from 20.2 to 23.85eV for crystalline films. The types of optical transition responsible for optical absorption are indirect allowed and direct forbidden transitions with energy gaps of 1.4 and 2.18eV for the amorphous films and of 1.38 and 2.33eV for the crystalline films, respectively.

P.K. Nair et.al [28] In this paper we present the basic concepts underlying the chemical bath deposition technique and the recipes developed in our laboratory during the past ten years for the deposition of good-quality thin films of CdS, CdSe, ZnS, ZnSe, PbS, SnS, $Bi_2S_3$, $Bi_2Se_3$, $Sb_2S_3$, CuS, CuSe etc. Typical growth curves, and optical and electrical properties of these films are presented. The effect of annealing the films in air on their structure and composition and on the electrical properties is notable: CdS and ZnS films become conductive through a partial conversion to oxide phase, CdSe becomes photosensitive, SnS converts to $SnO_2$, etc. The use of precipitates formed during deposition for screen printing and sintering, in polymer composites and as a source for vapor-phase deposition is presented. Some examples of the application of the films in solar energy related work are presented.

Revathi Naidu et.al [29] Researchers worldwide focus on new earth abundant and cheap absorber materials for use in thin film solar cells that allow wider use of photovoltaic in energy production. SnS is one of such promising absorber materials that comprises earth abundant elements (Sn, S). We describe here the effect of annealing of high vacuum evaporated(HVE) SnS thin films in vacuum and nitrogen atmosphere with relatively high pressures of nitrogen. SnS thin films with a thickness of 500 nm were deposited onto the surface of glass by HVE at a substrate temperature of 300 °C. The as-deposited SnS thin films were annealed at 500 °C

and 550 °C for 1 h in vacuum as well as in nitrogen with respect to ambient ($N_2$) pressure that varied in the range of 500–2000 mbar. We analyze crystalline quality, crystal structure, elemental and phase compositions, and electrical properties of SnS films before and after the annealing process and their changes. Our results show that the use of pressurized inert ambient, such as nitrogen, improves the crystalline quality as well as the electrical properties of SnS thin films. The enhanced growth of crystals and modification of micro-structural properties of SnS thin films as a function of annealing conditions (type of ambient, annealing temperature and ambient pressure) are discussed in detail.

A. Voznyi et.al [30] We demonstrate a simple approach to fabricate single-phase SnS thin films by thermal vacuum annealing of $SnS_2$layers obtained by the close-spaced vacuum sublimation method. It was found that the initial non-annealed $SnS_2$films exhibit typical chemical composition for $SnS_2$ with ratio of Sn/S = 0.49. The structural quality of the $SnS_2$phase was studied by X-ray diffraction and Raman spectroscopy measurements. In particular, it was established that films have a hexagonal 2H-$SnS_2$ crystal structure. The field emission scanning electron microscope analysis of the surface and cross-section shows plate-like crystallites with an average size of 2 μm. Annealing of the $SnS_2$samples was carried out at 300, 400, and 500 °C for 30, 60, and 90 min for each temperature, and at 600 °C for 30 min. It was shown that concentration of S gradually decreases with increasing annealing temperature and time. The samples annealed at 500 °C for 30, 60, and 90 min demonstrate a typical SnS composition ratio of Sn/S = 0.96. Further, by using X-ray diffraction, Raman, and energy dispersive X-ray analysis, we found that annealing of the samples at 500 °C for 30, 60, and 90 min provides a phase transition from hexagonal $SnS_2$to orthorhombic SnS. The shorter annealing time and temperature leads to the mixed SnS, $Sn_2S_3$, and $SnS_2$ phase composition. The shape and size of plate-like crystallites remains the same after annealing. However, randomly distributed nano-pores were observed. Transmittance and reflectance measurements of the $SnS_2$ and SnS films show both direct and indirect optical band gaps in the materials. For SnS films a large absorption coefficient of 104–105 cm−1 above the band gap was found. The current-voltage characteristic of the ITO/$SnS_2$/Sn structure shows small rectification current, while the current-voltage curve of ITO/SnS/Sn is linear. The dark resistivity was found to be 1.01 × 105 Ω cm and 1.18 × 103 Ω cm for $SnS_2$ and SnS films, respectively. The hetero-junction structure was obtained by annealing of the $SnS_2$ deposited on the ITO/CdS structure to obtain the SnS phase. The p-SnS/n-CdS hetero-junction shows weak photovoltaic response under illumination at AM

1.5 conditions, namely, open circuit voltage (Voc), short circuit current density (Jsc), and fill factor (FF) of 0.35 V, 34.08μA/$cm_2$, and 0.42, respectively.

Geoffrey K et.al [31] This paper describes a Transmission Line Model approach to the modeling and analysis of alloyed planar ohmic contacts. It briefly reviews the standard Transmission Line Model (TLM) commonly used to characterize a planar ohmic contact. It is shown that in the case of a typical Au-Ge-Ni alloyed ohmic contact, a more realistic model based on the TLM should take into account the presence of the alloyed layer at the metal semiconductor interface. In this paper, such a model is described. It is based on three layers and the two interfaces between them, thus forming a 'tri-Layer Transmission Line Model (TLTLM). Analytical expressions are derived for the contact resistance Rc and the contact end resistance *Re* of this structure, together with a current division factor, f. Values for the contact parameters of this TLTLM model are inferred from experimentally reported values of Rc and Re for two types of contact. Using the analytical outcomes of the TLTLM, it is shown that the experimental results obtained using a standard TLM can have considerable discrepancies.

K. Anuar et.al [32] Cathodic electro-deposition in the presence of EDTA in aqueous solution was used to prepare Cu2S thin film deposited on Ti substrate. The effect of deposition potential, concentration and deposition time was studied to determine the optimum condition for electro-deposition process. Cyclic voltammetry was performed to elucidate the electrodic processes that occur while potentials for electro-deposition were applied to determine the optimum potential for electro-deposition. The thin films are characterised by X-ray diffractometry. The photoactivity of the deposited films and their conduction types were evaluated using photo-electrochemical technique. The band gap energy and type of optical transitions were determined from optical absorbance data.

J. Proctor( member of IEEE) et.al [33] A four-terminal microelectronic test structure and test methods are described for electrically determining the degree of uniformity of the interfacial layer in metal-semiconductor contacts and for directly measuring the interfacial contact resistance. A two-dimensional resistor network model is used to obtain the relationship between the specific contact resistance and the measured interfacial contact resistance for contacts with a uniform interfacial layer. A new six-terminal test structure is used for the direct measurement of end contact resistance and the subsequent determination of front contact resistance. A methodology is described for reducing the effects of both contact-window mask misalignment and parasitic resistance associated with these measurements Measurement

results are given for 98.5-percent A1/1.5 percent Si and 100-percent A1 contacts on n-type silicon.

Biswajit Ghosh et.al [34] The electrical contact of metal–semiconductor (M–S) interface is normally evaluated using DC measurements like transfer of length model and volume transfer mode model. Preparation of these measurements needs high grade infrastructural facilities. Moreover, in the thin and nano-structure presences of surface states at the M–S interface perturb the dc results and led to the apparent conclusion. Influence of the surface states can be eliminated using the ac measurements. Considering M–S interface as a leaky capacitance a mathematical model has been developed in the present paper. Measuring M–S capacitance in three semiconducting films, e.g., n-Si, p-CdTe, and p-Cu2O and substituting these values in the developed model various parameters of the interface were evaluated. Results obtained by this method were compared with the results from dc measurements and these were comparable with each other. The scope of this

paper is the application of this method to the laboratories lacking in high grade infrastructure.

## 2.6 Conclusion

After going through these papers we have got the idea of SILAR process, its experimental procedure, crystallinity of SILAR based films, effect of different types of doping materials on the films, effect due to annealing and the properties of films fabricated by another processes like- vapour deposition, chemical bath deposition etc. However, we have encountered a gap of knowledge regarding the SILAR based films with varying cationic precursor to anionic precursor concentration ratio. So,we have chosen this work for our thesis.

# 3. SILAR PROCESS

## 3.1 Introduction

The Successive Ionic Layer Adsorption and Reaction (SILAR) method is basically a higher version of Chemical Bath Deposition process. It is comparatively newer and less experimented before. The main process of this method is immersion of substrate in cationic and anionic precursor solution and rinsing in de-ionised water in between them to obtain the growth of desired film. The basic difference between SILAR and CBD is growth mode. In CBD all the precursors are present at the same time in the reaction beaker, but in SILAR the substrate in separately rinsed in each precursor and this include immersion in de-ionised water in between them. As the rinsing isolates the individual steps, the growth of desired film takes place layer by layer. The thickness of the film is controlled directly by the number of the deposition cycles.

### Merits of SILAR

SILAR method is simple and it has lot of advantages over other processes. The advantages are listed below:

- We can easily control the thickness and deposition rate of the film n wide variation by changing the duration of rinsing and changing the number of cycles.
- Operates at room temperature.
- Unlike closed vapour deposition method, SILAR does not need high quality target or substrate and it does not need high vacuum at any stage.
- It is very easy process to dope film of any element by adding proportional amount of that element in cationic precursor solution.
- It does not cause local over heating that can be harmful for materials to be deposited.
- Less costly, simple and suitable for large area deposition.
- As the deposition is carried out at or close to room temperature there is less possibility of oxidation or corrosion of the metallic substrate.
- Since the basic deposition layers are ions instead of atoms, the preparative parameters are easily controlled with better orientation and improved grain structure can be obtained.

SILAR method has interesting feature and additional advantage over CBD method is that, SILAR method saves material cost due to non-formation of precipitate in solution. SILAR method can be used for the deposition from aqueous or non-aqueous baths and it can be employed in the preparation of polymers, semiconductors or oxides.

**Demerits of SILAR**

The drawbacks of this process are as follows:

- High total reaction time, which is up to several minutes in a cycle, is due to slow adsorption and rinsing which are affected by the diffusion times of the ions.
- A high pH value can cause problems with some pH sensitive substrate materials.

## 3.2 SILAR process description

The SILAR method is a relatively new and less investigated method, which is first reported in 1985 by Ristov et al. [35]. The name SILAR was ascribed to this method by Nicolau and Mernard (1985) and discussed in their subsequent papers [41], which deals with ZnS, CdZnS and CdS thin films. The SILAR method is useful for the deposition of thin films of chalcogenide groups such as I–VI, II–VI, III–VI, V–VI, VIII–VI binary and I–III–VI, II–II–VI, II–III–VI, II–VI–VI and II–V–VI ternary chalcogenides and composite films. SILAR process is intended to grow thin films of water insoluble ionic or ion compounds of the KpAa type by heterogeneous chemical reaction at the the solid solution interface between adsorbed cations pKa+ and anion aAp-, following reaction:-

$$pK^{a+}(aq) + qX^{b-}(aq) + b'Y^{q'+}(aq) + aA^{p-} \rightarrow KpAa(s) + qX^{b-}(aq) + b'Y^{q'+}(aq)$$

With ap = bq = b'q'.

where, 'K' represents cation (Cd2+, Pb2+, Zn2+, Fe3+, Cu+, etc.); 'p' represents the number of cations, a represents the numerical value of charge on cation, 'X' is an ion in cationic precursors having negative charge (X = $SO4^{2-}$, $Cl^{1-}$, $NO3^{1-}$etc.) q represents the number of X in cationic precursors and 'b' is the numerical value of charges on X. b' is the number of Y in the anionic solutions. q' is the numerical value of charge on Y, 'Y' is the ion which is attached to chalcogen ion, A represents the anion (O-, OH-, S, Se and Te),a is the number of anions.

The SILAR method is mainly based on the adsorption and reaction of the ions from the solutions and rinsing between every immersion with distilled water (D. W.) to avoid homogeneous precipitation in the solution.

Thin films have been obtained by adsorbed cations followed by reacting with anion from appropriate precursor solutions. The term "adsorption" can be defined as a collection of a substance on the surface of another substance, which is the fundamental building block of the SILAR method. Adsorption may be expected when two heterogeneous phases are brought in contact with each other. Hence, gas-solid, liquid-solid and gas-liquid are three possible adsorption systems. In SILAR method, the first step is mainly concern with adsorption in liquid-solid system. Adsorption is an exothermic process. The adsorption is a surface phenomenon between ions and surface of substrate and is possible due to attractive force between ions in the solution and surface of the substrate. These forces may be cohesive or Van-der Wall"s or chemical attractive. Atoms or molecules of their kinds on all sides do not surround atoms or molecules of substrate surface. Therefore, they possess unbalanced or residual force and hold the substrate particles. Thus, adsorbed atoms (ad-atoms) can be holding on the surface of the substrate. In second step the adsorbed ion is reacted with anion, resulted into film formation.

The SILAR method involves four steps:

1) Adsorption, 2) First rinsing, 3) Reaction and 4) Second rinsing

**1) Adsorption:-**

In first step of SILAR method, the cations present in the precursor solution are adsorbed on the surface of the substrate and form the Helmholtz electric double layer. This layer is composed of two layers: first, the inner (positively charged) and outer (negatively charged) layers. The positive layer consists of the cations and the negative form the counter ions of the cations.

**2) First rinsing:-**

In this step, loosely adsorbed ions are rinsed away from the diffusion layer. This results into saturated electrical double layer.

**3) Reaction:-**

In this reaction step, the anions from anionic precursor solution are introduced to the system. Due to the low stability of ions reaction between cation and anion takes place leading to formation of solid phase over substrate.

**4) Second rinsing:-**

In last step of SILAR method, the excess and unreacted species and the reaction by-product from the diffusion layer are removed. In this way, SILAR method culminated through adsorption of cations and reaction of newly adsorbed anions with pre-adsorbed cations, which leads to formation of thin film of desired material. The factors like temperature of solution, nature of the substrate, pH and concentration of solution, area of the substrate, dipping and rinsing time etc. affect the deposition process [36].

**3.5Effect of preparative parameters: -**

The rate of deposition and terminal thickness depends upon the adsorption and reaction time in the solution. In SILAR method, growth kinetics depends on the concentration of ions, adsorption and reaction time, rinsing time, temperature and on complexing agent. The effect of various deposition conditions on these parameters is discussed below.

**a) Concentration of ions**

The increase in compound concentration leads to an increase in cation and anion concentration and a film with larger thickness is obtained. Conversely, above a certain concentration of cation and anion when the rate of reaction becomes high and precipitation is leading to a lesser amount of material on the substrate then it lowers the thickness. Changing concentration of precursor solution, stoichiometry of the deposited material can be controlled.

**b) Adsorption and reaction time**

Adsorption and reaction time plays important role in formation of thin film. As the adsorption time is greater than that of reaction time the film formation takes place by assorted reaction it results higher terminal thickness. Equal adsorption and reaction time, result in to consistent reaction. Consistent growth provides uniform film formation.

**c) Rinsing time**

Rinsing between every immersion is significant to avoid the precipitation in the reaction bath. In rinsing bath the loosely bounded species peel off from the substrate surface. Sufficient rinsing time can provide a good quality film.

**d) Temperature**

The dissociation of complex and the anion of the compound depend on the temperature. At the higher temperatures, the dissociation is greater, which gives higher concentrations of cations and anions that result in higher rate of deposition.

### 3.3 Idea of solubility and Ionic product

When a sparingly soluble salt AB is dissolved in water. At equilibrium and saturated solution of $A^+$ & $B^+$ ions in contact with undissolved AB is obtained.

$$AB(S) \rightleftharpoons A+B$$

Applying law of mass action at equilibrium

$$K = \frac{[A^+][B^-]}{[AB]}$$

Where $[A^+]$,$[B^+]$,[AB] and K.

The concentration of pure solid phase is a constant.

$$K = \frac{[A^+][B^-]}{K'}$$

$$KK' = [A^+]\,[B^-].$$

$$K_s = [A^+]\,[B^-]$$

Where $K_s$ is solubility product and $[A^+]\,[B^-]$ is ionic product.

**For Saturated Solution:-**

$$K_s = [A^+]\,[B^-].$$

**For Supersaturated Solution:-**

$$K_s < [A^+]\,[B^-]$$

**For unsaturated Solution:-**

$$K_s > [A^+]\,[B^-]$$

The formation of solid phase from a solution includes two steps

i. Nucleation and
ii. Particle growth.

The size of particles of a solid phase is dependent upon the relatives rates at which these two competing process takes place. It also depends on temperature rate of mixing of precipitate during precipitation. A state of super saturation may be achieved by leaving the temperature of an unsaturated solution and formation of the solute at a fixed temperature. In highly supersaturated solution the rate of nucleation increases exponentially.

Rate of nucleation = $K_0$ (Q-S).

"Q" is the excess concentration above saturation and "S" is the concentration at saturation.

$(AB)_n + A^+ + B^- \rightarrow (AB)_{n+1}$

$(AB)_{n+1} + A^+ + B^- \rightarrow (AB)_{n+2}$.

Where, 'n' is the minimum no. of ions that must combine to yield the stable particle $(AB)_n$.

Rate of growth = $K_0$ (Q-S) A.

Where, A is the surface area of exposed solid '$K_0$' is the constant based on characteristic of particular precipitate.

If the saturation is maintained at low level throughout the precipitation, relatively few nuclei formed will grow to give a small no. of large particles. With high super saturation, many more nuclei are formed initially and nucleation may occur throughout the entire precipitation process and there will be so many centers of growth and none of the particles will become very large and a colloidal suspension is formed.

The growth kinetics of a thin film deposition consists of two types –

i. Ion by ion growth – ion by ion deposition at nucleation building block of in reversed surface.
ii. Cluster by cluster growth – Nucleation takes place by adsorption of the colloidal particles and growth takes place as a result of surface coagulation of these particles. This gives thin and adherent film.

## 3.4 Fabrication of SnS thin film using SILAR techniques

### 3.4.1 Cleaning of glass substrate

The cleanliness and hydrophilicity of glass substrate plays an important role for the growth of films. Contaminated substrate affects the growth and may leads to uneven distribution.

Here, we have used 7.6cm x 2.5cm x 0.1cm Glass slides as substrate.

- Glass substrate were washed with Acetone in Cotton.
- Cleaned in Ultrasonic vibrator for 110 min in an Ethanol : Water solution.
- Etched in HCl solution (37%) for 1 hour.
- Washed it thoroughly with running deionised water.
- Air dried and wrapped in Butter paper to avoid further contamination.

### 3.4.2 Preparation of Precursor solution

In the entire fabrication process we have prepared three sets of SnS thin films with varying concentration of Anionic precursor $Na_2S$ keeping the concentration of Cationic precursor constant in all three sets.

Cationic precursor solution – 250ml of 0.1N $SnSO_4$ solution with 6 to8 drops of $H_2SO_4$ to make pH nearly 1.8.

Anionic precursor solution – 250ml of 0.25N / 0.5N / 1N $Na_2S$ solution successively.

**Fig. 13.a Anionic Precursor, DW, Cationic Precursor, DW from left**

### 3.4.3 Fabrication procedure of Thin films

1) The cleaned dried Glass substrate is immersed and stirred continiously in Cationic precursor for 12s.
2) Then it is stirred in rinsing bath containing Distilled water for16s.
3) Further transferring and stirred in reaction bath containing Anionic precursor solution for 14s.
4) At last transferred and stirred again in another rinsing bath of Distilled water for 18s.
5) Then again it is transferred to adsorption bath containing Anionic precursor solution for next cycle.

This process is repeated up to 300 cycles to fabricate 4 samples of each set (3 sets).

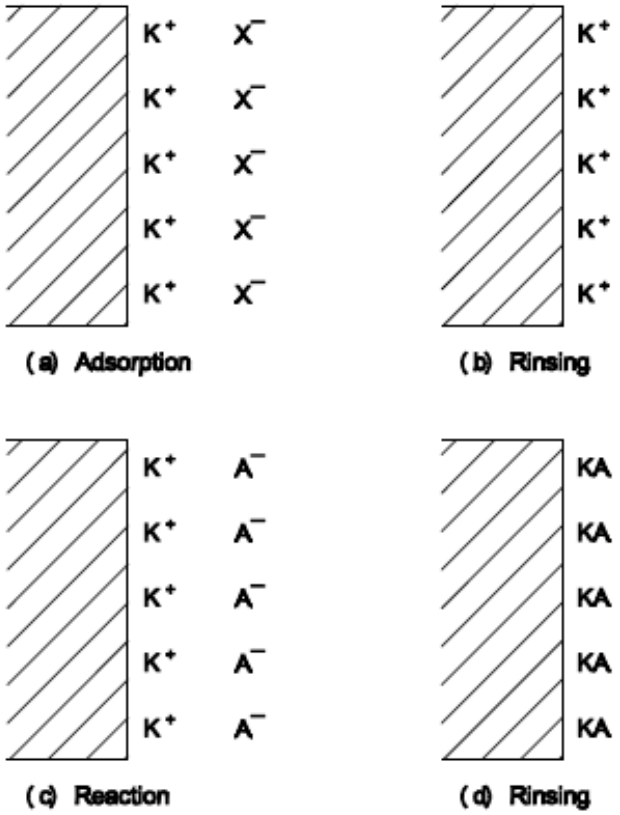


**Fig13.b**

### 3.5 Conclusion

In this chapter the whole fabrication process as well as the parameters affecting the deposition is discussed briefly. The time for adsorption, rinsing, reaction, rinsing has been optimised in initial steps of subsequent cycles. The time for adsorption and reaction is comparatively less than the rinsing time to avoid entangling of Sulphate or Sulphide ions in the films.

However, the deposited thin films were put to test its Chemical composition and structure which is described in the next chapter.

# 4. CHARACTERISATION OF SnS THIN FILMS

## 4.1 Introduction

## 4.2 X-ray diffraction(XRD)

The X-ray diffraction (XRD) is well known technique for characterisation of bulk and thin film samples. The structural identification and determination of lattice parameters are based on the interpretation of XRD patterns. It is non-destructive, non-contact and provides useful information, such as presence of phases, crystallite size and orientation and strain state. The phenomenon of XRD consists of reflection of X-rays from the different crystallographic planes of material. Fig. 15 and Fig. 16 show the image of X-ray diffractometer.

**Fig. 14**


**Fig. 15**

Diffraction in general occurs only when the wavelength of the wave motion is of the same order of magnitude as the repeat distance between scattering centres. This condition of diffraction is nothing but Bragg's law and is given by:-

$$2d \sin\theta = n\lambda$$

where, d = interplanar spacing, θ= glancing diffraction angle, n = order of diffraction (n = 1) and λ= wavelength of monochromatic X-ray, The detailed treatment of XRD analysis has been given in the literature [37, 38]. The Debye Scherrer's technique in conjunction with

diffractometer is most commonly used. In this instrument, the diffracted radiation is detected by the counter tube, which moves along the angular range of reflections. An inbuilt program on the computer system processes the observed intensities. A diffraction pattern consisting of d values of existing atomic planes in the sample and corresponding reflected intensities is made available from this XRD data following structural characterization can be carried out.

### 4.2.1 Identification of phases

The observed "d" values are compared with standard "d" values using Joint Committee on Powder Diffraction Standards (JCPDS) diffraction file or American Society for Testing Materials (ASTM) data card for the same material synthesized by standard chemical methods. This analysis reveals the different phases present in the sample and Miller indices of the atomic planes. The lattice parameters a, b and c for the unit cell of the phase present are then calculated using equations given by Kenon. The proportional amount of phases present can be determined from total intensities. Absence of reflection peaks indicates amorphous nature of the sample. A single reflection peak indicates an epitaxial growth, while many reflection peaks indicates heteroepitaxial (polycrystalline) growth. In case of a polycrystalline the average crystallite size is determined from Scherrer's formula [39].

$D = (K\lambda)/(\beta \cos\theta)$

Where D = Crystallite size, β= Corrected FWHM of the most intense peak, θ= Bragg's angle, K = constant

### 4.2.2 Determination of crystal structures

Crystal structure of a deposited material in bulk or thin film form determines the diffraction pattern of that material or more specifically the shape and size of the unit cell determines the angular positions of the diffraction lines and the arrangement of atoms within the unit cell along with the relative intensities of the lines.

The determination of an unknown structure proceeds in three major steps: -

Step I: The shape and size of the unit cell is deduced from the angular positions of the diffraction lines. First, an assumption is made to find out the unknown structure, which belongs to one of the seven crystal systems and then on the basis of this assumption, the correct Miller

indices are assigned to each reflection. This step is called “indexing the pattern” and is only possible, when the correct choice of crystal system has been made. Once this is done, the shape of the unit cell is known (from the crystal system) and its size is calculated from the position and Miller indices of the diffraction lines.

Step II: The number of atoms per unit cell is then computed from the shape and size of the unit cell.

Step III: Finally the positions of the atoms within the unit cell are deduced from the relative intensities of the diffraction lines.

## 4.3 FIELD EMISSION SCANNING ELECTRON MICROSCOPE|(FESEM)

### 4.3.1 Principle

Under vacuum, electrons generated by a field emission source (FES) are accelerated in a field gradient. The beam passes through electromagnetic lenses, focusing onto the specimen. As a result of this bombardment, different types of electrons are emitted from the specimen. A detector catches the secondary electrons and an image of the sample surface is constructed by comparing the intensity of these secondary electrons to the scanning primary electron beam.

Finally the image is displayed on a computer. The ray diagram of FE-SEM is shown in Fig. 17 and the ray diagram of emission of different types of electrons during scanning is shown in Fig. 18.

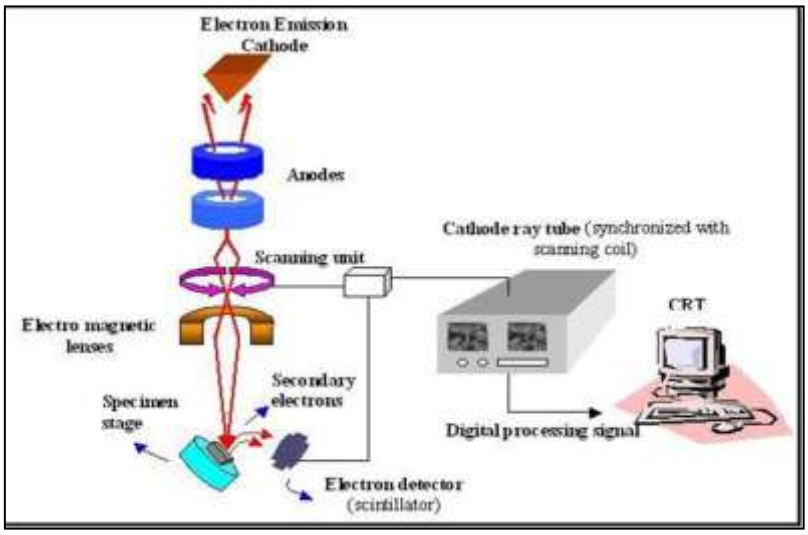


**Fig. 16**

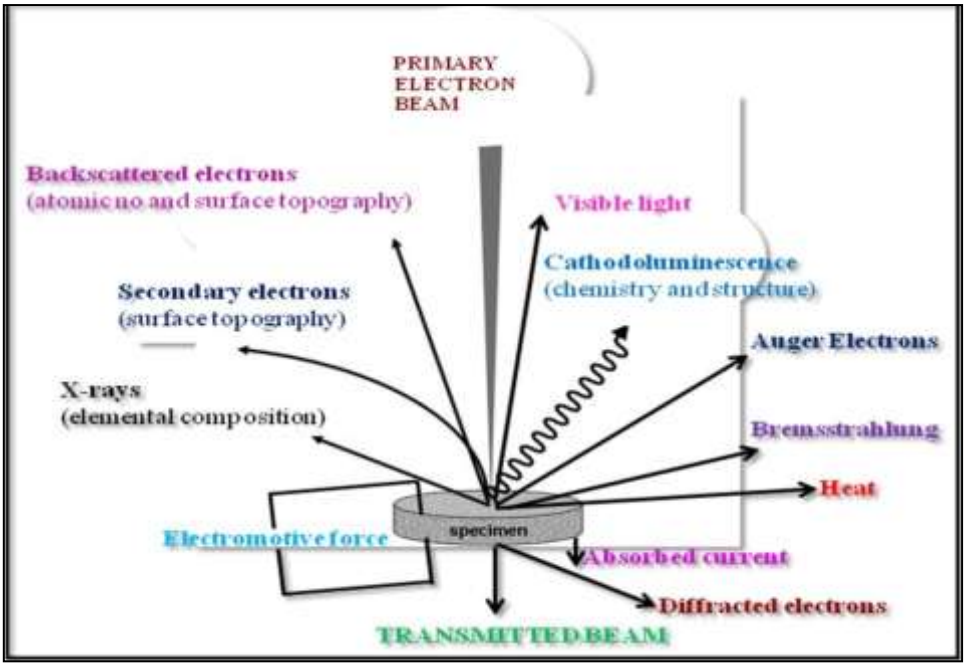


**Fig. 17**

### 4.3.2 Basic concepts

**(a) Vacuum**

The FE-SEM can be classified as a high vacuum instrument. The vacuum allows electron movement along the column without scattering and helps to prevent discharges inside the instrument. The vacuum design is a function of the electron source due to its influence on the cathode emitter lifetime.

**(b) Field emission source (FES)**

The function of the electron gun is to provide a large and stable current in a small beam. There are two classes of emission source: thermionic and field emitter. Emitter type is the main difference between the SEM and the FE-SEM. Thermionic emitters use electrical current to heat up a filament; the two most common materials used for filaments are tungsten (W) and lanthanum hexaboride ($LaB_6$). When the heat is enough to overcome the work function of the filament material, the electrons can escape from the material. Thermionic sources have relative low brightness, evaporation of cathode material and thermal drift during operation. Field emission is one of the ways of generating electrons that avoids these problems. A FES also called a cold cathode field emitter, which does not heat the filament. The emission is reached

by placing the filament in a huge electrical potential gradient. The significance of the small tip radius (~ 100 nm) is that an electric field can be concentrated to an extreme level. FE-SEM uses FES producing a cleaner image, less electrostatic distortions and spatial resolution < 2 nm (that means 3 or 6 times better than SEM). The FESEM (S-4800, Hitachi, Japan) (Fig. 2.7) has two anodes for electrostatic focusing. A voltage (0 ~ 6.3 KV) between the field emission tip and the first anode, called as the extraction voltage, controls the current emission (1 ~ 20 mA). A voltage (1 ~ 30 kV), called as the accelerating voltage, between the cathode and the second anode that increases the beam energy and determines the velocity at which the electrons move into the column. This voltage combined with the beam diameter determines the resolution (capacity to resolve two closely spaced points into two separates entities). As voltage increases, better point-to-point resolution can be obtained [40].

**(c) Electromagnetic lenses**

To resolve a feature on the specimen surface, the beam diameter must be smaller than the feature (still containing high current density). Therefore it is necessary to condense the electron beam. To assist in the demagnification of the beam, electromagnetic lenses are employed. Since, the cross over diameter in the FES is smaller, a lower level of the beam condensation is necessary to have a probe useful for image processing. This makes the FE-SEM as the highest resolution instrument.

**(d) Interaction Electron beam and specimen**

The specimen and the electron beam interact in both elastic and inelastic fashion giving different signals. Elastic scattering events are those that do not affect the kinetic energy of the electron even when its trajectory had been affected. Inelastic scattering events occur as a result of the energy transfer from the electron beam to the atoms in the specimen, as result the electrons have energy loss with small trajectory deviation. Some of the signals created in this way are: secondary electrons (SE), auger electrons and X-rays. Each of these signals gives specific information about topography, crystallography, surface characteristics, specimen composition and other properties.

## 4.4 ENERGY DISPERSIVE X-RAY SPECTROSCOPY (EDXS)

EDXS is also referred as EDS (Energy Dispersive Spectroscopy), EDXA (Energy Dispersive X ray Analysis). EDXMA (Energy Dispersive X-ray Microanalysis) or simply EDS. It is an analytical methodology to find out the elemental composition of the sample. It is done with X ray spectrum emitted by the sample bombarded with focussed beam of electrons to obtain the chemical composition. The number of X ray and the energy of X ray are the characteristic function of the difference in energy between the shells and the atomic structure of the elements from which they are emitted thus it makes the foundation to expose the chemical composition of the sample.

The composition so recorded or found is categorised as:-

1. Major components :-More than 10wt%
2. Minor components :-1-10wt%
3. Traces :-Below 1wt%

**Fig. 18 SEM machine**

# 5. RESULTS AND DISCUSSION

**Sample 1**

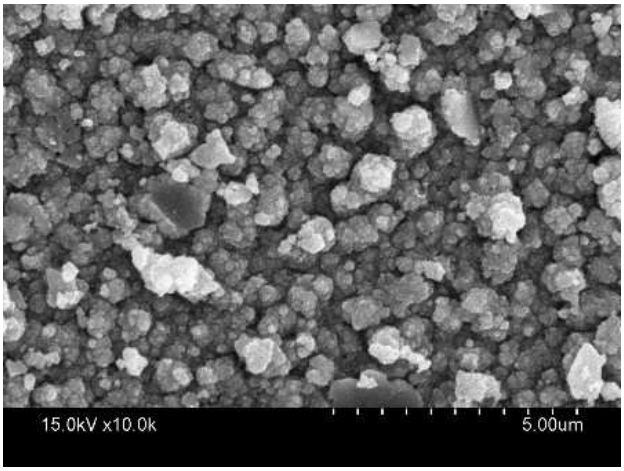


**(a) SEM1**

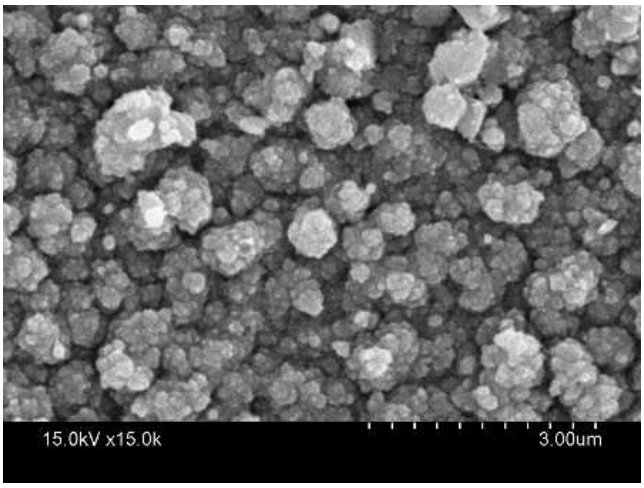


**(b)SEM2**

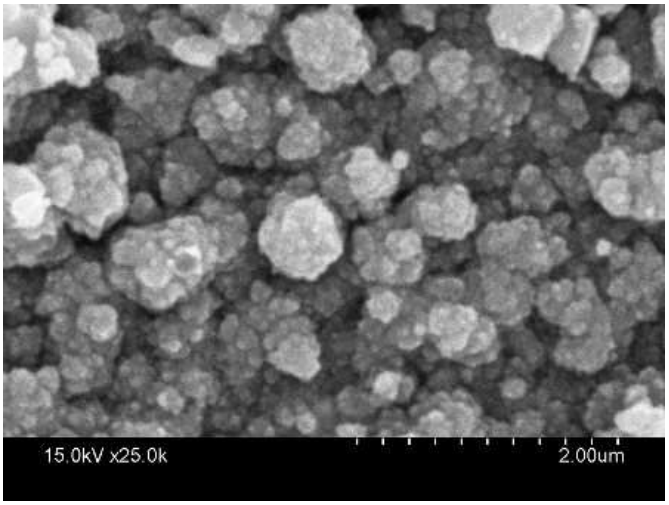


**(c)SEM3**

**Sample 2**

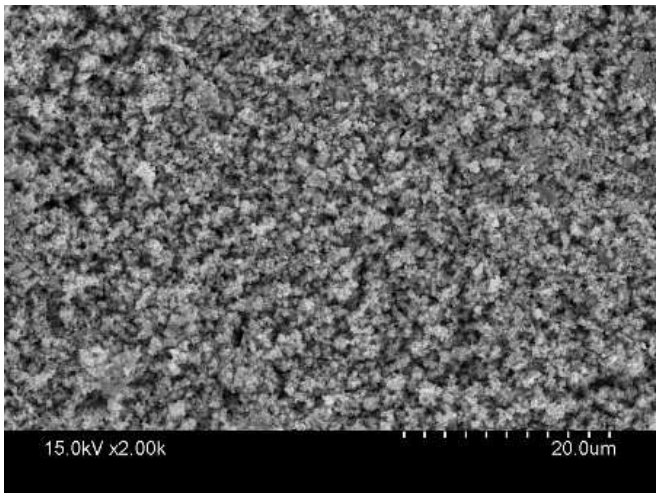


**(a) SEM1**

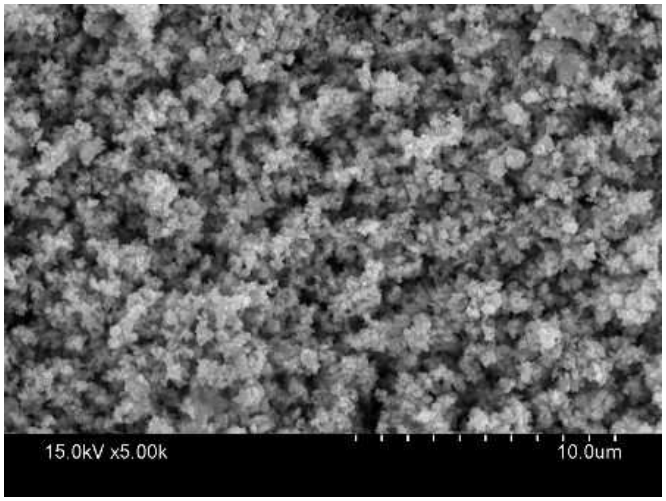


**(b) SEM2**

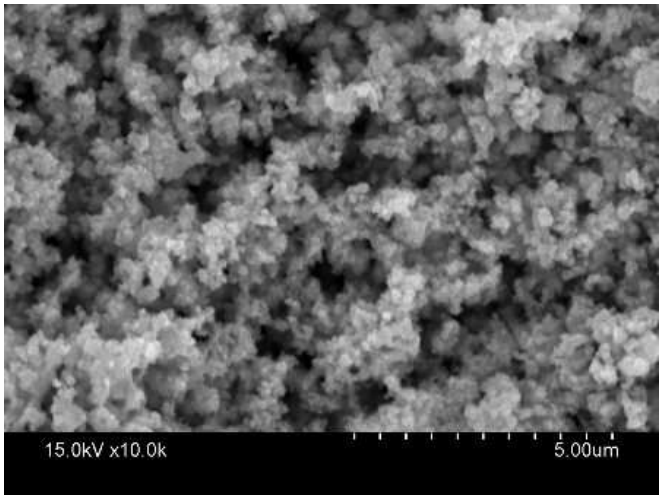


**(c) SEM3**

**SAMPLE 3**

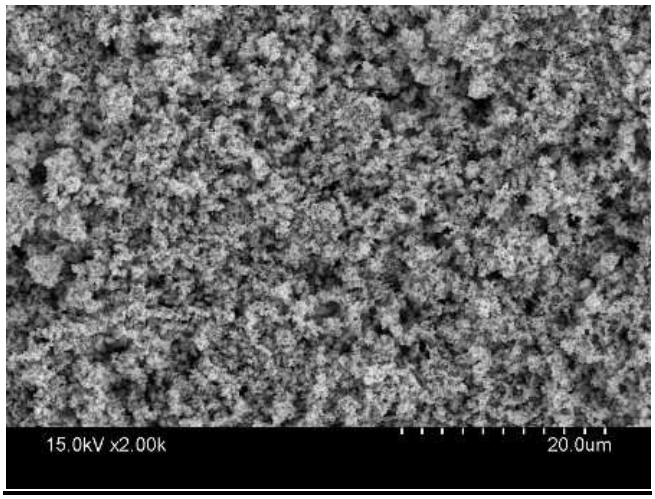


**(a) SEM1**

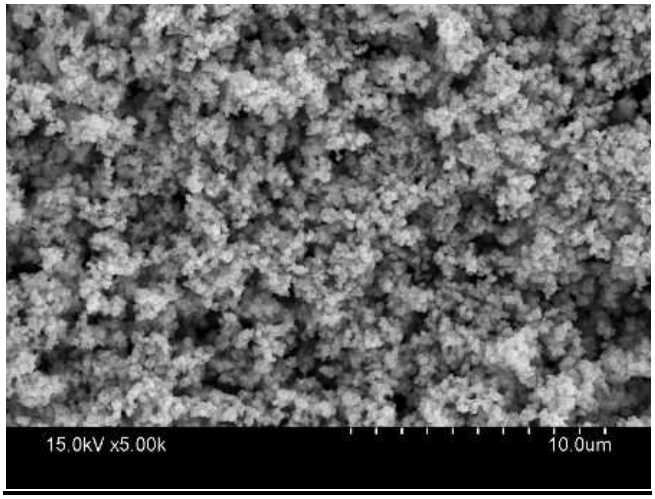


**(b) SEM2**

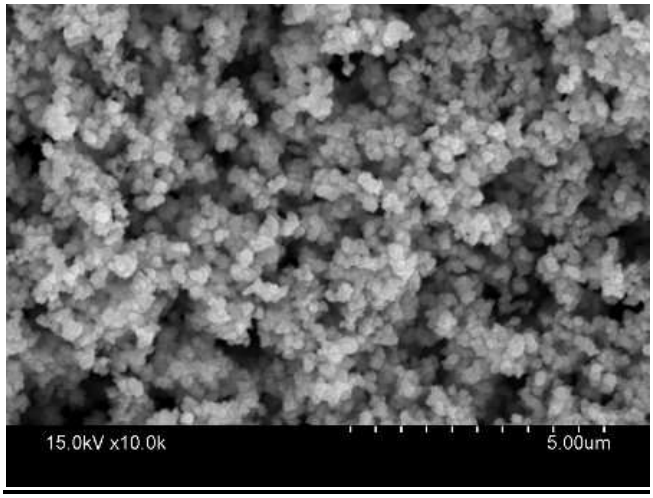


**(c) SEM3**

**SAMPLE 1**

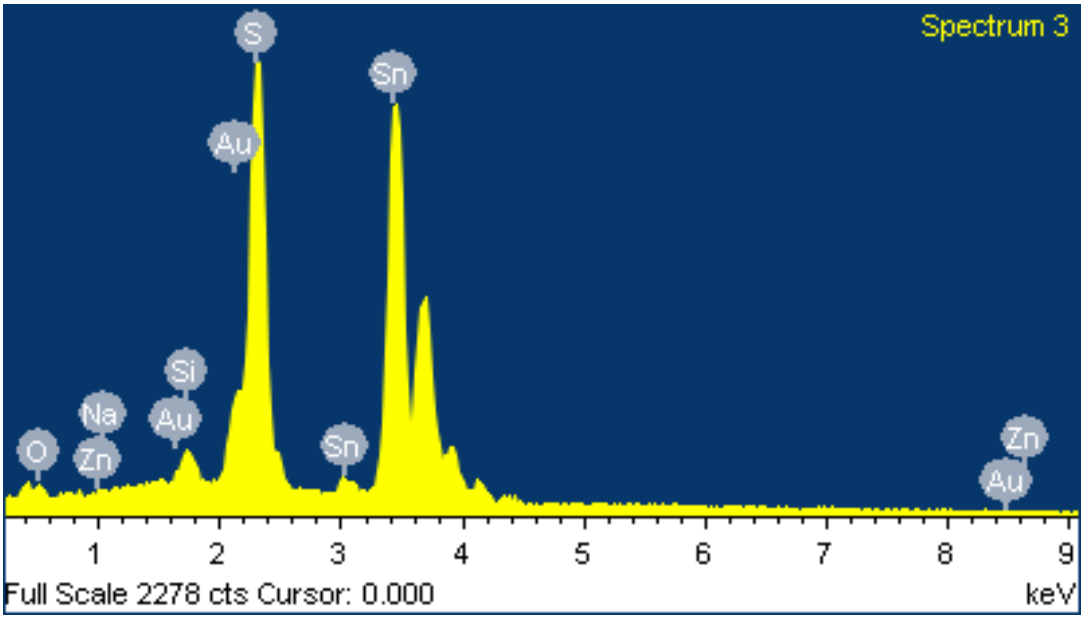


| Element | Weight% | Atomic% |
|---|---|---|
| O K | 3.82 | 16.40 |
| Na K | 0.02 | 0.06 |
| Si K | 1.16 | 2.83 |
| S K | 17.82 | 38.21 |
| Zn L | 0.38 | 0.40 |
| Sn L | 66.35 | 38.44 |
| Au M | 10.46 | 3.65 |
| Totals | 100.00 | |

**SAMPLE 2**

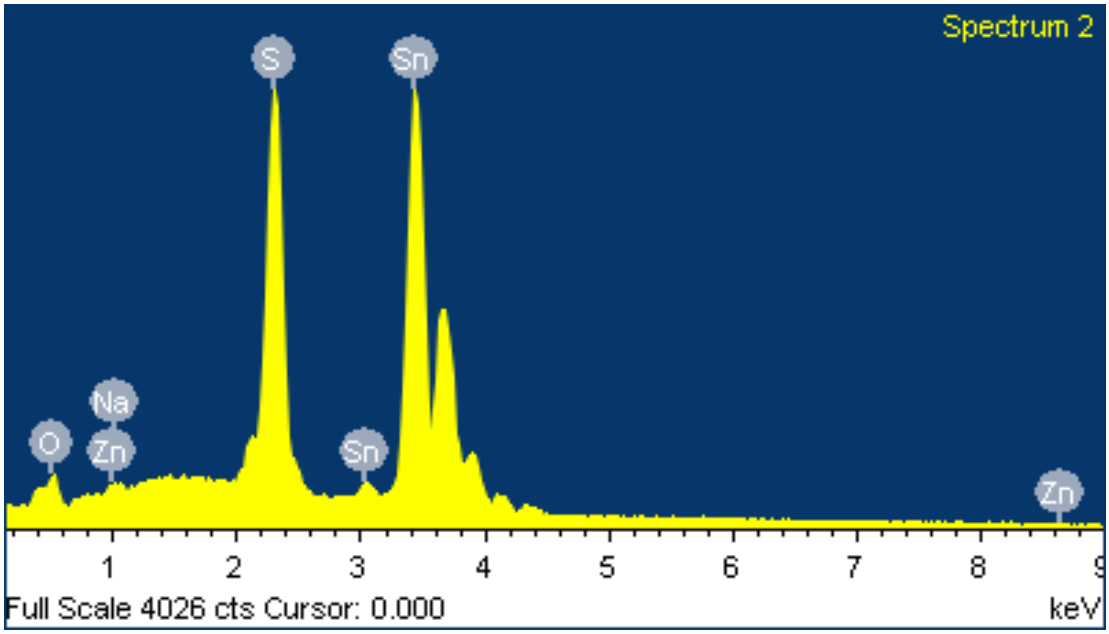


| Element | Weight% | Atomic% |
|---|---|---|
| O K | 9.24 | 33.09 |
| Na K | 0.42 | 1.05 |
| S K | 16.81 | 30.04 |
| Zn L | 0.79 | 0.69 |
| Sn L | 72.75 | 35.13 |
| Totals | 100.00 | |

**SAMPLE 3**

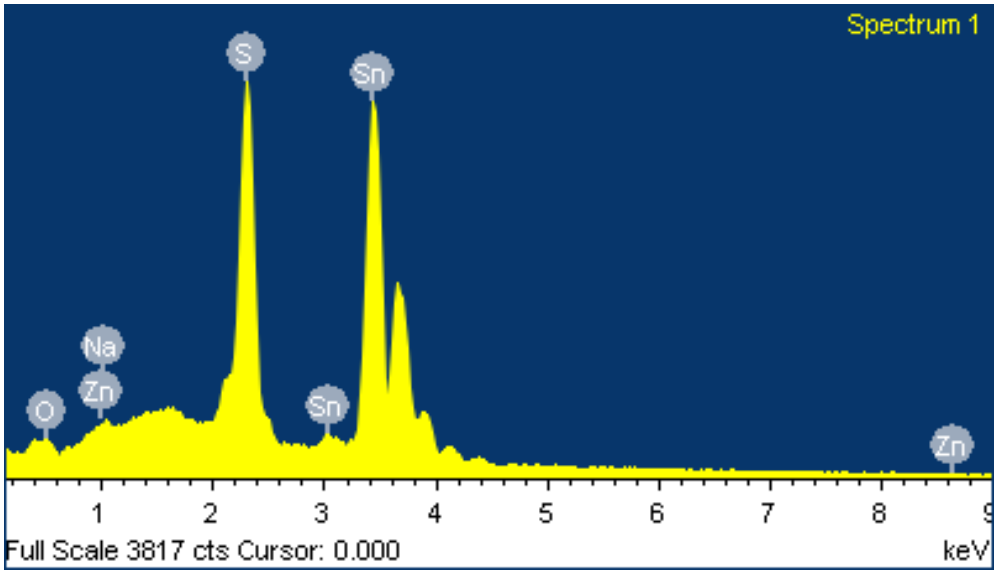


| Element | Weight% | Atomic% |
|---|---|---|
| O K | 5.91 | 23.48 |
| Na K | 0.33 | 0.91 |
| S K | 17.38 | 34.48 |
| Zn L | 0.49 | 0.47 |
| Sn L | 75.89 | 40.66 |
| Totals | 100.00 | |

## 5.1SEM & EDX Analysis

For qualitative analysis of chemical composition and structure EDX and SEM tests has been carried out. SEM images of all the samples shows that the deposition is pin hole free, strongly adherent to the glass substrate and blackish brown in appearance and they are of thickness in nanometric order. There is equal distribution of grain falling in Nanometer regime. Only in sample 2 and sample 3, It may be due to deliquescence nature of Tin Suphate, the samples have undergone cluster by cluster growth consequently due to high super saturation many more nucleic centers are formed and their growth process was hindered. Consequently as a result none of the particles can become very large and a colloidal suspension is formed. As far as the chemical composition is concerned, the EDX of three samples (1, 2, 3) with increasing anionic precursor concentration respectively (0.25N/0.5N/1N) the concentration of oxygen as one of impurities has shown a considerable growth due to absorption of moisture of Tin Sulphate while preparing latter two samples. Out of the three samples, all shows empirical ratio of Sn : S nearly 1.119.

Traces of Zn and Na are also found which may be present in raw chemicals. We can see a peak of Au in the right which is due to gold coating done for the test.

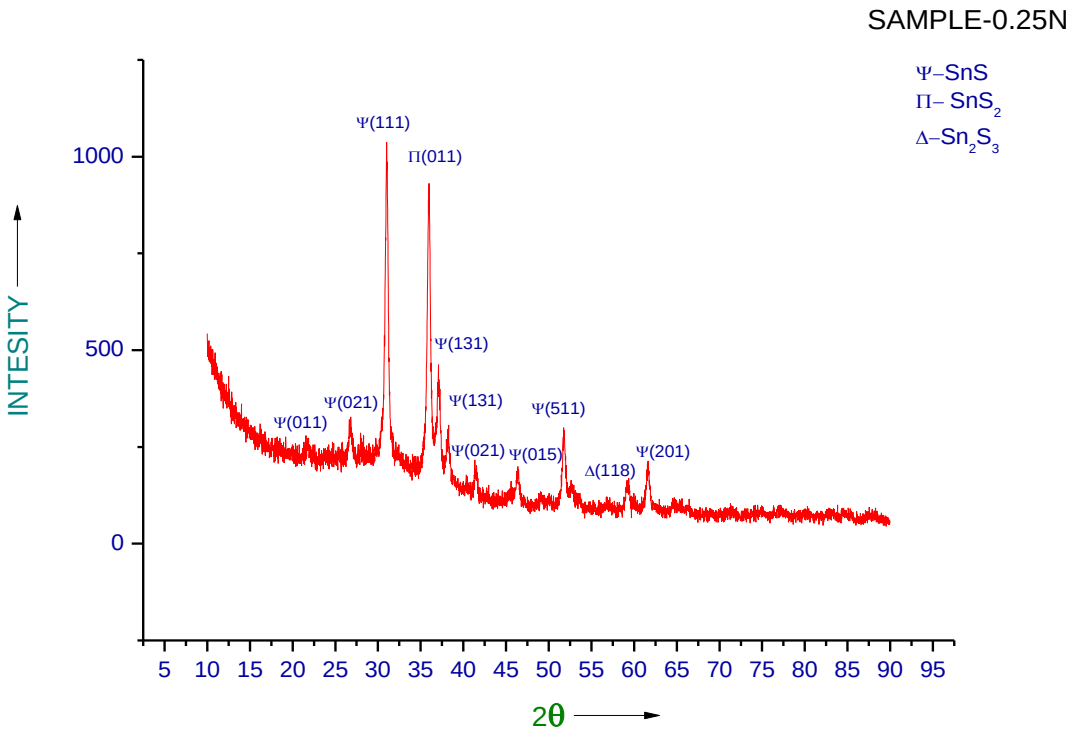


| 2θ | COMPOUND(LATTICE) | PDF NUMBER |
|---|---|---|
| **21.572** | SnS(011) | 750925 |
| **26.749** | SnS(021) | 831758 |
| **30.926** | SnS(111) | 831578 |
| **35.858** | $SnS_2$ (011) | 831707 |
| **37.1** | SnS(131) | 831758 |
| **38.569** | SnS(131) | 831578 |
| **41.279** | SnS(021) | 750925 |
| **46.45** | SnS(015) | 750925 |
| **51.877** | SnS(511) | 731859 |
| **59.275** | $Sn_2S_3$(118) | 752183 |
| **61.497** | $SnS_2$(201) | 831707 |

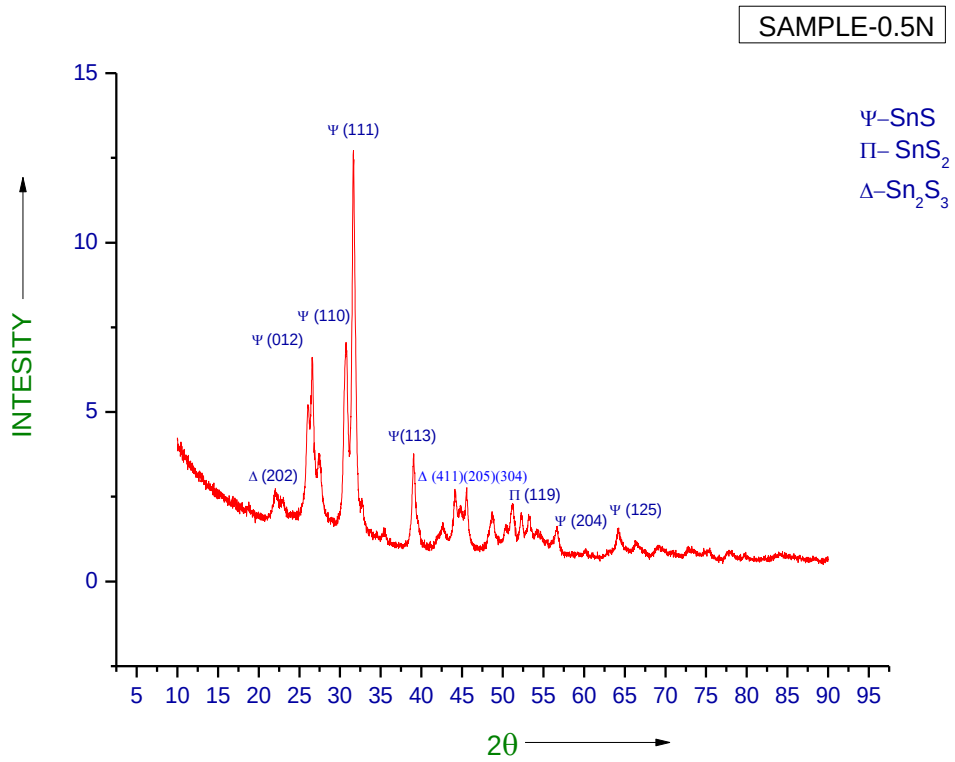


| 2θ | COMPOUND(LATTICE) | PDF NUMBER |
|---|---|---|
| **22.23** | $Sn_2S_3$(202) | 752183 |
| **26.647** | SnS(012) | 750925 |
| **30.726** | SnS(110) | 750925 |
| **31.65** | SnS(111) | 750925 |
| **39.078** | SnS(113) | 750925 |
| **48.769** | $Sn_2S_3$(411) | 752183 |
| **44.1** | $Sn_2S_3$(205) | 752183 |
| **45.47** | $Sn_2S_3$(304) | 752183 |
| **51.191** | $SnS_2$(119) | 401466 |
| **52.224** | $SnS_2$(119) | 401466 |
| **53.257** | $SnS_2$(119) | 401466 |
| **56.712** | SnS(204) | 750925 |
| **64.337** | SnS(125) | 750925 |

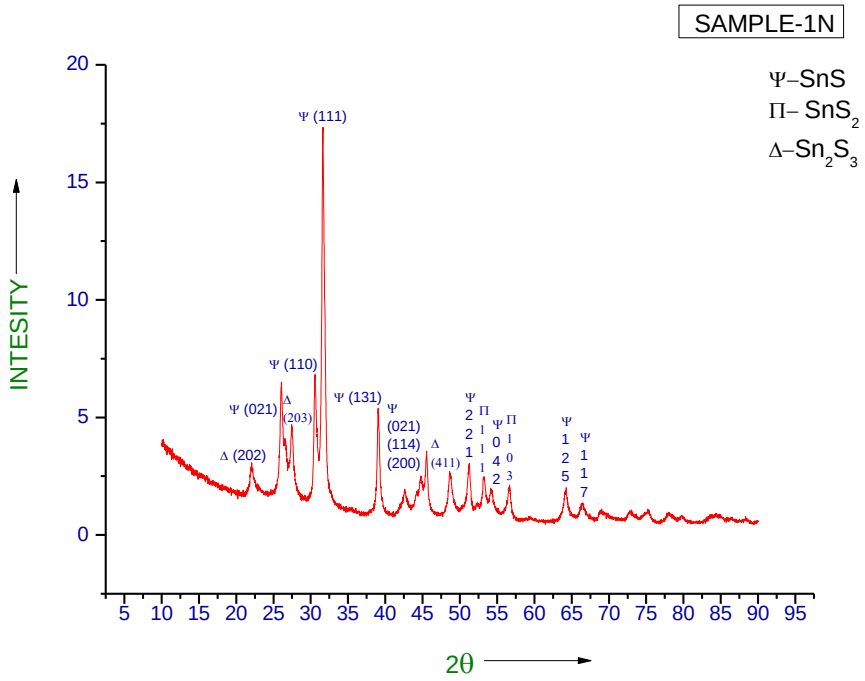


| 2θ | COMPOUND(LATTICE) | PDF NUMBER |
|---|---|---|
| **22.159** | $Sn_2S_3$(202) | 752183 |
| **26.131** | SnS(021) | 831758 |
| **27.521** | $Sn_2S_3$(203) | 752183 |
| **30.46** | SnS(110) | 750925 |
| **30.619** | SnS(110) | 750925 |
| **31.65** | SnS(111) | 831758 |
| **38.92** | SnS(131) | 831758 |
| **42.533** | SnS(021) | 750925 |
| **44.638** | SnS(114) | 750925 |
| **45.472** | SnS(200) | 750925 |
| **48.848** | $Sn_2S_3$(411) | 752183 |
| **51.191** | SnS(221) | 831758 |
| **53.256** | $SnS_2$(111) | 831707 |
| **54.289** | SnS(042) | 831758 |
| **56.712** | $SnS_2$(103) | 831706 |
| **64.178** | SnS(125) | 750925 |
| **66.402** | SnS(117) | 750925 |

## 5.2 XRD Analysis

XRD was carried out in two different machines: sample1 in a machine of make PHILIPS ANALYTICAL X-RAY B.V LELYWEG 1 7602EA ALMEIO of target material cobalt and sample 2 and 3 was tested in a D8 ADVANCE machine of target material copper.

XRD depicts that the film so deposited polycrystalline structure. The peaks are matched with JCPDS cards according to the target material. It is found that the most dominant peak was of SnS with orthorhombic structure with lattice indices <111> around 2θ nearly 36°-37° in all the samples which is the most preferential crystalline growth plane. With respect to the intensities of the most dominant peak the intensities of other peaks are found and matched with JCPDS cards. It is obvious that traces of $SnS_2$ and $Sn_2S_3$ are present with SnS. Their peaks are also clear and distinct showing different lattice planes mentioned in the table shown above. These peaks are distributed in the entire 2θ range of 10°-90° on either side of the dominant peak along with some other peaks of SnS in the XRD graph.

## 5.3 Conclusion

Due to scarcity of time and non-availability of test facilities in our own campus we have gone through three tests (SEM, EDS, XRD) only. The overall results of these tests revealed that the SILAR process up to the mark and got our work accomplished in accordance with the fixed benchmarks. All the films deposited shown clear and distinctive peaks of SnS, $SnS_2$, $Sn_2S_3$.The SEM confirms the growth without any pin hole and EDX imparts the chemical composition assuring traces below nominal level.

# 6. CONCLUSION

## 6.1 Summary of the work

Here, we have gone through the variation of anionic precursor and three compositional and structural tests (SEM, EDX, XRD) only due to lack of time.

XRD results show the Bragg's peaks confirm the polycrystalline nature of the films. SEM and EDX shows the depositions are free from pin hole with fine grains size and of nanometric range of thickness. The deposition of film with varying concentration of tin sulphate can also be tried for more accurate and better optimization. Ten the entire work can be pushed in a sequential pattern into further steps of optimization to withstand the SnS material in commercial module which is the most alarming and thrived area in research.

## 6.2 Concluding Remarks

This work describes the SILAR process and fabrication of SnS thin films with variation of sodium sulphide only. While performing the experiments some precautionary measures should be taken like:

a) The raw materials to be used should be extra pure.

b) They should be kept and preserved in a pollution free environment as tin sulphide is deliquescent in nature.

c) Substrate should be cleaned properly.

d) The time for adsorption and reaction should be kept lees than half of rinsing.

e) The deposition should be carried out in a clean space with special care.

The electrical characteristics of the films should also be explored to match its suitability with preferred choices.

## 6.3 Avenues for the future work

It is the prior responsibility of researcher to convey the information of investigation so they can be put into practical application to tackle the problems and swipe the contemporary drawbacks and use these findings to sustain commercialization more firmly.

Fabrication of SnS thin films with varying Sn : S is one of the most alarming field of research. In this work, only varying concentration of anionic precursor is done. The work can be extended further with varying concentration of cationic precursor so that the optimization process can be introduced at the grass root level then proceeding for further optimization with complex agent, doping and multiple doping, annealing at different stages. This judicious sequence to go step by step will surely place SnS as window layer in commercial module in parallel confrontation with Si.

However, in the first step we have observed the clear success in polycrystalline deposit of SnS with fine grains. Besides ,these we should also go for exploration of electrical characteristics and more improved and modern tests like FESEM, HRSEM, HRTEM, Raman Spectroscopy to get more information about surface morphology, grain size, particle size, structural defects, chemical composition, presence of defective bands, band gap (direct and indirect).

# REFERENCES


[1] Sohila S., Rajalakshmi M., Muthamizhchelvan C.et. al. Synthesis and characterization of SnSnanosheets through simple chemical Routes. Materials Letters 65 (2011) 1148–1150

[2] El-Nahass M.M., Zeyada H.M., Aziz M.S..et. al. Optical properties of thermally evaporated SnS thin films. Optical Materials 20 (2002) 159–170

[3] Basak Arindam, HatiArjyabha, MondalAnup et.al. Effect of substrate on the structural, optical and electrical properties of SnS thin films grown by thermal evaporation method.

Thin Solid Films 645 (2018) 97–101

[4] BasakaArindam, MondalaAnup, Singh Udai P. et.al. Impact of substrate temperature on the structural, optical and electrical properties of thermally evaporated SnS thin films. Materials Science in Semiconductor Processing 56 (2016) 381–385

[5] GhoshBiswajit, BhattacharjeeRupanjali, Das Subrata et.al. Structural and optoelectronic properties of vacuum evaporated SnS thin films annealed in argon ambient. Applied Surface Science 257 (2011) 3670–3676

[6] Reddy N. Koteeswara., et al. Electrical properties of spray pyrolytic tin sulfide films. Solid-State Electronics 49 (2005) 902–906

[7] Patel Malkeshkumar, MukhopadhyayIndrajitet. al. Molar optimization of spray pyrolyzedSnS thin films for photoelectrochemical applications. Journal of Alloys and Compounds 619 (2015) 458–463

[8] Sajeesh T.H., Warrier Anita R. et. al. Optimization of parameters of chemical spray pyrolysis technique to get n and p-type layers of SnS. Thin Solid Films 518 (2010) 4370–4374

[9] Rana Tanka Raj, Kim SeongYeonet. al. Existence of multiple phases and defect states of SnS absorber and its detrimental effect on efficiency of SnS solar cell. Current Applied Physics 18 (2018) 663–666

[10] Patel Malkeshkumar, MukhopadhyayIndrajit et.al. Annealing influence over structural and optical properties of sprayed SnS thin films Optical Materials 35 (2013) 1693–1699

[11] Mathews N.R., Garcia C. Colin et. al. Effect of annealing on structural, optical and electrical properties of pulse electrodeposited tin sulfide films. Materials Science in Semiconductor Processing 16 (2013) 29–37

[12] OgahOgah E., Reddy Kotte Ramakrishna et.al. Annealing studies and electrical properties of SnS-based solar cells. Thin Solid Films 519 (2011) 7425–7428

[13] Chalapathi U., Poornaprakash B. et.al. Effect of post-deposition annealing on the growth and properties of cubic SnS films. Superlattices and Microstructures 103 (2017) 221-229

[14] GhoshBiswajit, Das Madhumita, Das Subrataet.al.Characteristics of metal/p-SnSSchottky barrier with and without post-deposition annealing. Solid State Sciences 11 (2009) 461–466

[15] Ghosh B., Das M., Das S. et.al. Fabrication of vacuum-evaporated SnS/CdSheterojunction for PV applications Solar Energy Materials & Solar Cells 92 (2008) 1099– 1104.

[16] Das .R S, vankar .D .V, N. Premand Chopra .L. K .et al. thepreparation of $Cu_2S$ films for solar cells. Thin Solid Films, 51 (1978) 257-264.

[17] Salman .A .K .et al. Effect of surface texturing processes on the performance of crystalline silicon solar cell. Solar Energy 147 (2017) 228–231.

[18] Kul**.** M .et al. Electrodeposited SnS film for photovoltaic applications. Vacuum 107 (2014) 213-218.

[19] Arulanantham .S .M .A, Valanarasu.S ,Jeyadheepan .K, Ganesh .V,Shkir .M .et al. Development of SnS (FTO/CdS/SnS) thin films by nebulizer spray pyrolysis (NSP) for solar cell applications .Journal of Molecular Structure 1152 (2018) 137-144.

[20] N. R. Koteeswara, M. Devika, R. K. Gunasekhar .et al. Stable and low resistive zinc contacts for SnS based optoelectronic devices. Thin Solid Films 558 (2014) 326–329.

[21] Hara.O .K, S .Shinto ,Usami .N.et al. Formation of metastable cubic phase in SnS thin films fabricated by thermal evaporation. Thin Solid Films 639 (2017) 7–11.

[22] G. Furao, G. Huafei , Z. Kezhi, YuanNingyi , Ding Jianning.et al. Variations in structural and optoelectronic features of thermally co-evaporated SnS films with different Sn contents. Thin Solid Films 642 (2017) 285–289.

[23] Andrade-Arvizua .A .Jacob,García-Sánchezb .F.M, Agudeloa-Pulgarin .F.Courel-Piedrahitaa .M, Jaimesa-Santiago .E, Resendiza-Valencia .E,Plazac-Arce .A, O. Galán-Vigil .O.et al. Suited growth parameters inducing type of conductivity

conversions on chemical spray pyrolysis synthesized SnS thin films. Journal of Analytical and Applied Pyrolysis 121 (2016) 347–359.

[24] Ghosh.B .et al. Work function engineering and its applications in ohmic contact fabrication to II–VI semiconductors. Applied Surface Science 254 (2008) 4908–4911.

[25] Sun lili, Zhou Wei, LiuYanyun, YuDandan, LiangYinghu , Eu Ping.et al. Theoretical perspective on the electronic, magnetic and opticalproperties of Zn-doped monolayer $SnS_2$. Applied Surface Science 389 (2016) 484–490.

[26] Hegde.S.S, Kunjomana .G.A,Chandrasekharan.A.K,Ramesh.K, Prashantha.M.et al. Optical and electrical properties of SnS semiconductor crystals grown by physical vapor deposition technique. Physica B 406 (2011) 1143–1148.

[27] El-Nahass .M.M, Zeyada .M.H, Aziz .S.M, El-Ghamaz .A.Net al. Optical properties of thermally evaporated SnS thin films. Optical Materials 20 (2002) 159–170.

[28] Nair .K.P, Nair .S.T.M, GarcIa .M.V, Arenas .L.O, Pena.Y, Castillo .A, Ayala .T.I, Gomezdaza .O, Sanchez .A, Campos .J,Hu .H, Suarez .R, Rincon .E.M.et al**.** Semiconductor thin films by chemical bath deposition for solar energy related applications. Solar Energy Materials and Solar Cells 52 (1998) 313-344.

[29] N.Revathi, Loorits .M, Kärber .E, Volobujeva .O, RaudojaJaan, M .Natalia ,B.Sergei, Mellikov Enn.et al**.** Impact of vacuum and nitrogen annealing on HVE SnS photo-absorber films. Materials Science in Semiconductor Processing 71 (2017) 252–257.

[30] Voznyi .A, Kosyak .V, Grase .L, Vecstaudža .J, Onufrijevs .P, Yeromenko .Yu, Medvid .A, Opanasyuk .A.et al**.** Formation of SnS phase obtained by thermal vacuum annealing of SnS2 thin films and its application in solar cells. Materials Science in Semiconductor Processing 79 (2018) 32–39.

[31] Reeves .K.Gand Harrison .B.H.et al**.**An Analytical Model for Alloyed OhmicContactsUsing a Trilayer Transmission Line Model.IEEE TRANSACTIONS ON ELECTRON DEVICES, VOL. 42,NO.8.AUGUST 1995.

[32] Anuar .K, Zainal .Z, Hussein .Z.M, Saravanan .N, Haslina .Iet al. Cathodicelectrodeposition of Cu2S thin film forsolar energy conversion. Solar Energy Materials & Solar Cells 73 (2002) 351–365.

[33] Proctor J.S (member, IEEE),Linhom .W.L (member, IEEE).et al. Direct Measurements of Interfacial Contact Resistance, End Contact Resistance, and Interfacial Contact Layer Uniformity. IEEE TFLANSACTIONS ON ELECTRON DEVICES, VOL. ED-30, NO. **11,** NOVEMBER 1983.

[34] Ghosh.B(Member, IEEE), and M.Ratan.et al. Evaluation of Electrical contact in thin semiconducting films from AC Measurements. *ELECTRON DEVICES SOCIETY, Digital Object Identifier 10.1109/JEDS.2016.2563520.*

[35] Ristov M., Sinadinovskia G, et.al. Thin Solid Films 123(1985) 63.

[36] Pathan H, Lokhande C, Mater.Bull.et.al. Sci. 27 (2004) 15.

[37] U. Welzel, J. Ligot, P. Lamparter, A. C. Vermeulen, E. J. Mittemeijer,J. Appl. Cryst. 38 (2005) 1.

[38] J. L. Van Heerden and U. R. Swanepoel, Thin Solid Films 299 (1997)72.

[39] Marotti R, Giorgi P.et.al. Sol. Energy Mater. Sol. Cells 90 (2006) 2356.

[40] Epifani M, Zamani R .et.al.Thin Solid Films 555 (2014) 39.

[41] Nicolau Y , Mernard J, Cryst J.et.al. Growth 92 (1988) 128.

[42] Gratzel M, Inorg. Chem. 44 (2005) 6841.

[43] Gratzel M, Acc. Chem. Res. 42 (2009) 1788.

[44] Serrano E, Rus G, Martinez J, Renew Sust. Energy Rev. 13(2009) 2373.

[45] Rand D. Solid State Electrochem. 15 (2011) 1579.

[46] Fu J. L, Liu H, Holze R, Solid State Sci. 8 (2006) 113.

[47] Spallart M, J. Electrochem. Soc. 145 (1998) 337.

[48] D. M. Mattox, "Handbook of Physical Vapour Deposition (PVD) Processing", William Andrew. (2010).